

Classification of symmetric periodic trajectories in ellipsoidal billiards

BY PABLO S. CASAS* AND RAFAEL RAMÍREZ-ROS*

December 13, 2011

We find and classify nonsingular symmetric periodic trajectories (SPTs) of billiards inside nondegenerate ellipsoids of \mathbb{R}^{n+1} . SPTs are defined as periodic trajectories passing through some symmetry set. We prove that there are exactly $2^{2^n(2^{n+1}-1)}$ classes of such trajectories. We have implemented an algorithm to find minimal SPTs of each of the 12 classes in the 2D case (\mathbb{R}^2) and each of the 112 classes in the 3D case (\mathbb{R}^3). They have periods 3, 4 or 6 in the 2D case; and 4, 5, 6, 8 or 10 in the 3D case. We display a selection of 3D minimal SPTs. Some of them have properties that cannot take place in the 2D case.

Smooth convex billiards are a paradigm of conservative dynamics, in which a particle collides with a fixed closed smooth convex hypersurface of \mathbb{R}^{n+1} . They provide examples of different dynamics: integrable, mostly regular, chaotic, etc. In this paper we tackle the integrable situation. Concretely, we find and classify symmetric periodic trajectories (SPTs) inside ellipsoids of \mathbb{R}^{n+1} . PTs show different dynamics, which describe how they fold in \mathbb{R}^{n+1} . STs present symmetry with regard some coordinate subspace of \mathbb{R}^{n+1} . Dynamics and symmetry are precisely the main aspects we consider in our classification of SPTs. We establish 112 classes of SPTs in the 3D case, and we find a representative of each class with the smallest possible period. Those minimal SPTs have periods 4, 5, 6, 8, or 10. We depict a selection of minimal 3D SPTs. Some of them have properties that cannot take place in the 2D case. SPTs are preserved under symmetric deformations of the ellipsoid. In a future paper we plan to study their bifurcations and the transition between stability and instability under such deformations.

1 Introduction

Smooth convex billiards, in which a point particle moves uniformly until it undergoes abrupt elastic collisions with a smooth strictly convex hypersurface $Q \subset \mathbb{R}^{n+1}$, are one of the typical examples of conservative systems with both regular and chaotic dynamics. The 2D case ($n = 1$) was introduced by Birkhoff [4] and there is an extensive literature about it. The high-dimensional case remains much less studied, although we highlight two known results. First, a Nekhoroshev-like theorem for billiards was established in [20]. Second, some general lower bounds on the number of periodic billiard trajectories can be found in [2, 15, 16, 17]. Of course, these lower bounds are not informative for integrable systems, where periodic trajectories are organized in continuous families.

Only ellipsoids are known to be integrable smooth convex billiards and an old conjecture of Birkhoff states that this should be the sole case. The conjecture remains still unproven, but Berger [3] and Gruber [21] proved that only ellipsoids have caustics when $n \geq 2$, which is a powerful argument for the conjecture. A *caustic* is a smooth hypersurface with the property that a billiard trajectory, once tangent to it, stays tangent after every reflection.

Periodic trajectories (PTs) are the most distinctive trajectories, so their study is the first task. There exist two remarkable results about PTs inside ellipsoids: *Poncelet theorem* and *Cayley conditions*. Poncelet [26] showed that if a billiard trajectory inside an ellipse is periodic, then all the trajectories sharing its conic caustic are also periodic. Cayley [6] gave some algebraic conditions for determining conic caustics whose trajectories are periodic. Later on, both results were generalized to any dimension in [9, 12].

Almost all papers on billiards inside ellipsoids follow an algebro-geometric approach to the problem [1, 7, 8, 9, 11, 12, 13, 18, 25, 30]. Recently, a more dynamical approach to billiards inside ellipsoids has been considered in [5, 14, 31, 32]. We follow that approach, in which the description of the dynamics is more important than the obtaining of explicit formulae. Indeed, this paper is a natural continuation of the study on (minimal) periodic trajectories carried out in [5]. In the framework of smooth convex billiards the minimal period is always two. Nevertheless, since all the two-periodic billiard trajectories inside ellipsoids are singular—in the sense that some of their caustics are singular elements of a family of confocal quadrics—, two questions arise. Which is the minimal period among nonsingular billiard trajectories? Which ellipsoids display such trajectories? The authors settled both questions in [5].

Our current goal is to find and classify all symmetric periodic trajectories (SPTs) inside nondegenerate ellipsoids. We also look for minimal SPTs—representatives of each class with the smallest possible period.

Roughly speaking, a symmetric trajectory (ST) inside

$$Q = \left\{ (x_1, \dots, x_{n+1}) \in \mathbb{R}^{n+1} : \frac{x_1^2}{a_1} + \dots + \frac{x_{n+1}^2}{a_{n+1}} = 1 \right\},$$

*. Departament de Matemàtica Aplicada I, Universitat Politècnica de Catalunya, Diagonal 647, 08028 Barcelona, Spain (pablo@casas.upc.es, Rafael.Ramirez@upc.edu). The first author was supported in part by MCyT-FEDER grant MTM2006-00478 (Spain). The second author was supported in part by MICINN-FEDER Grant MTM2009-06973 (Spain) and CUR-DIUE Grant 2009SGR859 (Catalonia).

is a billiard trajectory invariant under a reflection with respect to some of the $2^{n+1} - 1$ coordinate proper subspaces of the Euclidean space \mathbb{R}^{n+1} . For instance, the left trajectory in Fig. 1 is invariant under the x_1 -axial and x_1x_3 -specular reflections, whereas the right one is invariant under the x_2 -axial reflection. There are twice as many “billiard symmetries” as coordinate proper subspaces of \mathbb{R}^{n+1} . This is easily understood by means of the following example. We can associate two different kinds of SPTs to any axis of coordinates of \mathbb{R}^{n+1} ; namely, the ones with an impact point on the axis and the ones with a segment parallel to the axis. Note that the left SPT in Fig. 1 has an impact point on the x_1 -axis —and so, it is invariant under the x_1 -axial reflection—, but also has a segment parallel to the x_2 -axis —and so, it is invariant under the x_1x_3 -specular reflection. We will check that this kind of double symmetry is the norm among SPTs, not the exception.

In view of the above arguments it is easy to guess that there is a rich casuistry of SPTs inside nondegenerate ellipsoids of \mathbb{R}^{n+1} , so much so that there is no simple way to describe them. For simplicity, let us briefly consider the 3D case: $n = 2$. Then, any billiard trajectory inside $Q \subset \mathbb{R}^3$ has two caustics of the form

$$Q_\lambda = \left\{ (x_1, x_2, x_3) \in \mathbb{R}^3 : \frac{x_1^2}{a_1 - \lambda} + \frac{x_2^2}{a_2 - \lambda} + \frac{x_3^2}{a_3 - \lambda} = 1 \right\}.$$

Let us assume that $0 < a_1 < a_2 < a_3$. We restrict our attention to nonsingular trajectories. That is, trajectories whose caustics are ellipsoids: $0 < \lambda < a_1$; 1-sheet hyperboloids: $a_1 < \lambda < a_2$; or 2-sheet hyperboloids: $a_2 < \lambda < a_3$. The singular values $\lambda \in \{a_1, a_2, a_3\}$, are discarded. It is known that there are only four types of couples of nonsingular caustics: EH1, H1H1, EH2, and H1H2. The notation is self-explanatory. It is also known that each caustic type gives rise to a different billiard dynamics. For instance, only trajectories with EH2-caustics rotate around the x_3 -axis. The left trajectory in Fig. 1 is a sample.

Coming back to the general case, its billiard trajectories present 2^n different caustic types, which describe how trajectories fold in \mathbb{R}^{n+1} ; see [5]. Then, we classify SPTs inside nondegenerate ellipsoids of \mathbb{R}^{n+1} , by their caustic types and their symmetries. That is, two SPTs with the same symmetries, but different caustic type, are in different classes. On the one hand, not every symmetry takes place among SPTs of a given caustic type, but only 2^{n+1} . On the other hand, all SPTs are, in some sense, doubly

symmetric, which rise to $2^n(2^{n+1} - 1)$ the classes we may encounter with a given caustic type. Consequently, we know that there are at most $2^{2n}(2^{n+1} - 1)$ classes of SPTs. Finally, by means of an argument involving *winding numbers*, we establish the existence of SPTs for all those classes.

That concludes the analytical part of the work. We have also implemented a numerical algorithm to find minimal SPTs of each of the 12 classes in the 2D case, and each of the 112 classes in the 3D case. They have periods 3, 4 or 6 in the 2D case; and 4, 5, 6, 8 or 10 in the 3D case. We depict all 2D minimal SPTs in Table 5, and just a gallery (for brevity of exposition) of 3D minimal SPTs in Sec. 6.

For instance, we show in Fig. 1 two minimal SPTs of period 6, but with only 5 and 4 different impact points. Only the second phenomena can take place in the 2D case. This has to do with the fact that, from a generic point on the ellipsoid, we can trace four lines tangent to a fixed couple of caustics. On the contrary, we can trace just two in the 2D case.

Some of the ideas used in this paper were first introduced by Kook and Meiss [22], to classify symmetric periodic orbits of some standard-like reversible $2n$ -dimensional symplectic maps. The technical details of our problem are harder —there are more symmetries, caustic types play a role, and the classification does not depend only on the evenness or oddness of some integers—, but the main arguments do not change.

Some of our billiard SPTs could be considered as discrete versions of the closed geodesics on triaxial ellipsoids found in [19]. For instance, it is interesting to compare the SPT on the left side of Fig. 1 with the symmetric closed geodesic shown in Fig. 4 of that paper. Of course, the SPT on the right side of Fig. 1 have no continuous version, because there are no geodesics with return points.

We complete this introduction with a note on the organization of the article. We review the classical theory of reversible maps in Sec. 2 following the survey [24]. Next, we specialize that theory to billiards inside symmetric hypersurfaces. In Sec. 4 we review briefly some well-known results about billiards inside ellipsoids, in order to fix notations that will be used along the rest of the paper. Billiards inside ellipses of \mathbb{R}^2 and inside triaxial ellipsoids of \mathbb{R}^3 , are thoroughly studied in Sec. 5 and Sec. 6, respectively. Billiards inside nondegenerate ellipsoids of \mathbb{R}^{n+1} are revisited in Sec. 7. Perspectives and conclusions are drawn in Sec. 8.

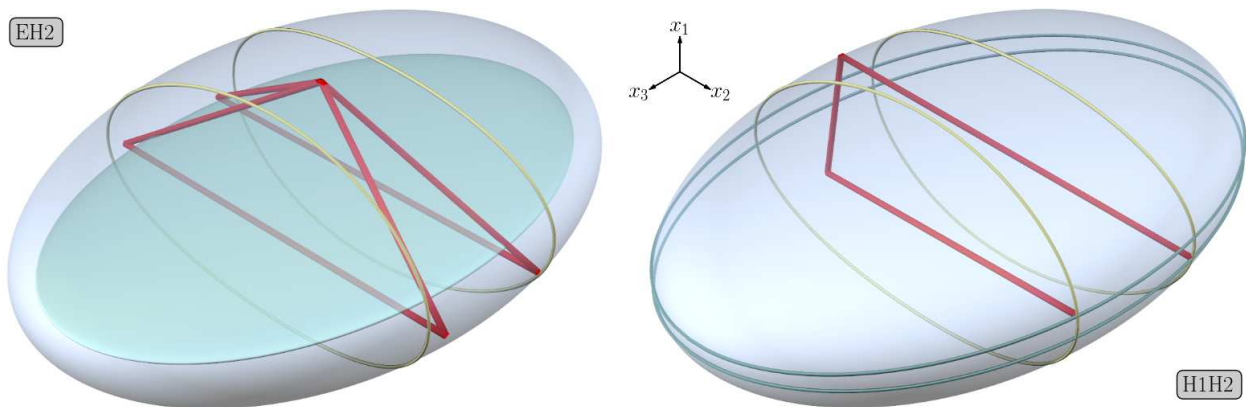


Figure 1. Two SPTs of period 6, but with only 5 and 4 different impact points. Lines in green and yellow represent the intersections of the ellipsoid with H1-caustics and H2-caustics, respectively. The E-caustic is also shown in the EH2 figure.

2 Reversible maps and symmetric orbits

In this section we state the concept of symmetric periodic orbit for a map. A map is reversible if each orbit is related to its time reverse orbit by a symmetry transformation. Reversible maps can be characterized as maps that factorize as the composition of two involutions. Symmetric orbits must have points on certain symmetry sets; namely, the fixed sets of the involutions (reversors) which factorize the original map. A reversible map can have different factorizations and, therefore, its symmetric orbits can be classified according to the symmetry sets they intersect.

Let $f: M \rightarrow M$ be a diffeomorphism on a manifold M .

Definition 1. *The map f is symmetric when there exists an involution $s: M \rightarrow M$ (i.e. $s \circ s = I$), such that $f \circ s = s \circ f$. Then, s is called a symmetry of the map f .*

Definition 2. *The map f is reversible when there exists an involution $r: M \rightarrow M$ such that $f \circ r = r \circ f^{-1}$. Then, r is called a reversor of the map f (i.e. f is r -reversible).*

Remark 1. The composition of a symmetry and a reversor (provided both commute) is another reversor.

Definition 3. *If r is a reversor, we denote by $\text{Fix}(r) = \{m \in M: r(m) = m\}$ its set of fixed points, which is called the symmetry set of the reversor.*

Definition 4. *An orbit of the map f is a sequence $O = (m_j)_{j \in \mathbb{Z}}$ such that $m_j = f(m_{j-1}) = f^j(m_0)$.*

Definition 5. *An orbit O of a r -reversible map f is called r -symmetric when $r(O) = O$.*

The following characterization of reversible maps goes back to G. D. Birkhoff.

Lemma 1. *A map f is reversible if and only if it can be factorized as the composition of two involutions, in which case both of them are reversors of f .*

Proof. Let us assume that f is \tilde{r} -reversible. Then $\hat{r} = f \circ \tilde{r} = \tilde{r} \circ f^{-1}$ is another reversor, because:

- $f \circ \hat{r} = f \circ \tilde{r} \circ f^{-1} = \hat{r} \circ f^{-1}$, and
- $\hat{r}^2 = \hat{r} \circ \hat{r} = \tilde{r} \circ f^{-1} \circ f \circ \tilde{r} = \tilde{r}^2 = I$.

Therefore, the map $f = f \circ \tilde{r}^2 = \hat{r} \circ \tilde{r}$ is the composition of two involutions.

On the other hand, if $f = \hat{r} \circ \tilde{r}$ and $\hat{r}^2 = \tilde{r}^2 = I$, then:

- $f \circ \tilde{r} \circ f = \hat{r} \circ \tilde{r}^2 \circ \hat{r} \circ \tilde{r} = \hat{r}^2 \circ \tilde{r} = \tilde{r}$, and
- $f \circ \hat{r} \circ f = \hat{r} \circ \tilde{r} \circ \hat{r}^2 \circ \tilde{r} = \hat{r} \circ \tilde{r}^2 = \hat{r}$,

so both involutions \hat{r} and \tilde{r} are reversors of the map f . \square

The factorization of a reversible symmetric map as a composition of two involutions is not unique. From any given factorization $f = \hat{r} \circ \tilde{r}$, we can construct infinitely many more, namely, $f = \hat{r}_k \circ \tilde{r}_k$, where $\hat{r}_k = f^{k+1} \circ \tilde{r} = f^k \circ \hat{r} = \hat{r} \circ f^{-k}$ and $\tilde{r}_k = f^k \circ \tilde{r}$ for any $k \in \mathbb{Z}$. Nevertheless, these new factorizations do not provide new symmetric orbits, because $\hat{r}(O) = \tilde{r}(O) = \hat{r}_k(O) = \tilde{r}_k(O)$, i.e., an orbit is invariant under \tilde{r} (or \hat{r}) if and only if it is invariant under all the reversors \tilde{r}_k and \hat{r}_k . On the contrary, the existence of a symmetry s commuting with the reversors \tilde{r} and \hat{r} is more promising, because then $f = (s \circ \tilde{r}) \circ (s \circ \hat{r})$ is a new factorization, which could give rise to new kinds of symmetric orbits. The more such symmetries exist, the more kinds of symmetric orbits we can try to find.

Given a factorization $f = \hat{r} \circ \tilde{r}$, we say that \tilde{r} and \hat{r} are *associated reversors*, and $\text{Fix}(\tilde{r})$ and $\text{Fix}(\hat{r})$ are *associated symmetry sets*. The importance of these concepts is clarified in the following characterization of symmetric orbits, which can be found in [24].

Theorem 1. *Let $f = \hat{r} \circ \tilde{r}$ be any factorization of a reversible map as the composing of two involutions. Then an orbit of this map is:*

- a) \hat{r} -symmetric if and only if it is \tilde{r} -symmetric.
- b) \tilde{r} -symmetric if and only if it has at least one point on $\text{Fix}(\tilde{r}) \cup \text{Fix}(\hat{r})$, in which case it has no more than two points on $\text{Fix}(\tilde{r}) \cup \text{Fix}(\hat{r})$.
- c) \tilde{r} -symmetric and periodic if and only if it has exactly two points on $\text{Fix}(\tilde{r}) \cup \text{Fix}(\hat{r})$, in which case it has a point on each symmetry set if and only if it has odd period. In particular,
 - i. An orbit is \tilde{r} -symmetric with period $2k$ if and only if it has a point m_* such that either $m_* \in \text{Fix}(\tilde{r}) \cap f^k \text{Fix}(\tilde{r})$ or $m_* \in \text{Fix}(\hat{r}) \cap f^k \text{Fix}(\hat{r})$, in which case $f^k(m_*)$ is on the same symmetry set as m_* .
 - ii. An orbit is \tilde{r} -symmetric orbit with period $2k + 1$ if and only if it has a point m_* such that $m_* \in \text{Fix}(\tilde{r}) \cap f^k \text{Fix}(\hat{r})$, in which case $f^{k+1}(m_*) \in \text{Fix}(\hat{r})$.

Proof. This is an old result, so we skip most of the details. We focus in those aspects that are more relevant for our goals.

- a) It is immediate as $\hat{r}(O) = \tilde{r}(O)$.
- b) To begin with, let us assume that an orbit $O = (m_j)_{j \in \mathbb{Z}}$ is \tilde{r} -symmetric, so there exists some $l \in \mathbb{Z}$ such that $m_l = \tilde{r}(m_0)$. Then $m_{l+1} = f(m_l) = \hat{r}(m_0)$, because $\hat{r} = f \circ \tilde{r}$. We distinguish two cases:

- If $l = 2k$ is even then $m_k \in \text{Fix}(\tilde{r})$ as:

$$m_k = f^{-k}(m_{2k}) = f^{-k}(\tilde{r}(m_0)) = \tilde{r}(m_k).$$

- If $l = 2k + 1$ is odd then $m_{k+1} \in \text{Fix}(\hat{r})$ as:

$$\begin{aligned} m_{k+1} &= f^{-(k+1)}(m_{2k+2}) \\ &= f^{-(k+1)}(\hat{r}(m_0)) = \hat{r}(m_{k+1}). \end{aligned}$$

On the other hand, let us assume that O has a point, say m_k , in one of those fixed sets. Then there exist two possibilities. In the case $m_k \in \text{Fix}(\tilde{r})$, $\forall j \in \mathbb{Z}$:

$$m_{k+j} = f^j(m_k) = f^j(\tilde{r}(m_k)) = \tilde{r}(f^{-j}(m_k)) = \tilde{r}(m_{k-j}).$$

In the case $m_k \in \text{Fix}(\hat{r})$, from $\tilde{r} = f^{-1} \circ \hat{r}$, $\forall j \in \mathbb{Z}$:

$$\begin{aligned} m_{k+j-1} &= f^{j-1}(m_k) = f^{j-1}(\hat{r}(m_k)) \\ &= f^j(\tilde{r}(m_k)) = \tilde{r}(f^{-j}(m_k)) = \tilde{r}(m_{k-j}). \end{aligned}$$

Hence, O turns out to be \tilde{r} -symmetric in both cases.

- c) Next, we study the symmetric periodic orbits. First, if O has two points, say m_0 and m_k , on $\text{Fix}(\tilde{r})$, then O is $2k$ -periodic, because:

$$\begin{aligned} m_{2k} &= f^k(m_k) = f^k(\tilde{r}(m_k)) \\ &= \tilde{r}(f^{-k}(m_k)) = \tilde{r}(m_0) = m_0. \end{aligned}$$

Second, if O has one point on each symmetry set, say $m_0 \in \text{Fix}(\tilde{r})$ and $m_{k+1} \in \text{Fix}(\hat{r})$, then O is $(2k+1)$ -periodic, because:

$$\begin{aligned} m_{2k+1} &= f^k(m_{k+1}) = f^k(\hat{r}(m_{k+1})) \\ &= f^{k+1}(\tilde{r}(m_{k+1})) = \tilde{r}(f^{-(k+1)}(m_{k+1})) \\ &= \tilde{r}(m_0) = m_0. \end{aligned}$$

□

Therefore, the computation of symmetric orbits with period $2k$ can be reduced to the computation of points on symmetry sets, which are mapped onto the same symmetry set after k iterations of the map. On the other hand, the computation of symmetric orbits with period $2k+1$ can be reduced to the computation of points on symmetry sets, which are mapped onto their associated symmetry sets after $k+1$ iterations of the map.

3 Billiards on symmetric hypersurfaces of \mathbb{R}^{n+1}

Let Q be a (strictly) convex smooth hypersurface of \mathbb{R}^{n+1} . The billiard motion inside Q can be modelled by means of a diffeomorphism f defined on the *phase space*

$$M = \{(q, p) \in Q \times \mathbb{S}^n : p \text{ is directed outward } Q \text{ at } q\}.$$

We define the *billiard map* $f: M \rightarrow M$, $f(q, p) = (q', p')$, as follows. The new velocity p' is the reflection of the old one p , with respect to the tangent hyperplane $T_q Q$. That is,

$$p' = p_t - p_n = p - 2p_n,$$

where p_t and p_n are the tangent and normal components at q of the old velocity:

$$p = p_t + p_n, \quad p_t \in T_q Q, \quad p_n \in N_q Q. \quad (1)$$

Let $q + \langle p' \rangle$ be the line through q with direction p' . Then the new impact point q' is determined by the condition

$$Q \cap (q + \langle p' \rangle) = \{q, q'\}.$$

That is, q' is the intersection of the ray $\{q + \mu p' : \mu > 0\}$ with the hypersurface Q . This intersection is unique and transverse by convexity.

Definition 6. A *billiard orbit* is a sequence of points $\{m_j\}_{j \in \mathbb{Z}} \subset M$ such that $m_j = f(m_{j-1}) = f^j(m_0)$. If the points $m_j = (q_j, p_j)$ form a billiard orbit, then the sequence of impact points $\{q_j\}_{j \in \mathbb{Z}} \subset Q$ is a *billiard (or impact) configuration*, whose joining by polygonal lines form a *billiard trajectory*; the sequence of outward velocities $\{p_j\}_{j \in \mathbb{Z}} \subset \mathbb{S}^n$ is a *velocity configuration*.

The distinction between orbits and trajectories is clear. We refer to orbits when we are working in the phase space M , whereas we refer to trajectories when we are drawing in \mathbb{R}^{n+1} . There exists an one-to-one correspondence between billiard orbits and billiard configurations. The velocities of the billiard orbit that correspond to the billiard configuration $\{q_j\}_{j \in \mathbb{Z}}$ are:

$$p_j = \frac{q_j - q_{j-1}}{|q_j - q_{j-1}|}. \quad (2)$$

From now on we shall assume that the hypersurface Q is symmetric with regard to *all* coordinate hyperplanes of \mathbb{R}^{n+1} . Then the billiard map admits 2^{n+1} factorizations as a composition of two involutions. We need the following notations in order to describe them.

Let Σ be the set made up of the *reflections* —that is, involutive linear transformations— with respect to the 2^{n+1} coordinate subspaces of \mathbb{R}^{n+1} . We represent its elements as diagonal matrices whose diagonal entries are equal to 1 or -1 , so

$$\Sigma = \{\sigma = \text{diag}(\sigma_1, \dots, \sigma_{n+1}) : \sigma_j \in \{-1, 1\} \text{ for all } j\}.$$

Given $(q, p) \in M$, there exists a unique point \hat{q} such that

$$Q \cap (q + \langle p \rangle) = \{q, \hat{q}\}.$$

Thus, \hat{q} denotes the previous impact point. Finally, let \tilde{p} be the reflection of the velocity p with respect to the normal line $N_q Q$. That is,

$$\tilde{p} = -p' = p_n - p_t = p - 2p_t,$$

where p_t and p_n were defined in the decomposition (1).

In what follows, symbols q' , p' , \hat{q} , and \tilde{p} have the meaning given in the previous paragraphs. We emphasize that they make sense only after both impact point q , and unitary outer velocity p , are given. Next we describe the 2^{n+1} factorizations of the billiard map.

Proposition 1. Let $f: M \rightarrow M$, $f(q, p) = (q', p')$, be the billiard map inside a closed convex symmetric hypersurface $Q \subset \mathbb{R}^{n+1}$. Let $\tilde{r}, \hat{r}: M \rightarrow M$ be the maps

$$\tilde{r}(q, p) = (q, \tilde{p}), \quad \hat{r}(q, p) = (\hat{q}, -p).$$

Let $s_\sigma, \tilde{r}_\sigma, \hat{r}_\sigma: M \rightarrow M$ be the maps

$$s_\sigma(q, p) = (\sigma q, \sigma p), \quad \tilde{r}_\sigma = s_\sigma \circ \tilde{r}, \quad \hat{r}_\sigma = s_\sigma \circ \hat{r}$$

for any reflection $\sigma \in \Sigma$. Then:

- a) $f = \hat{r} \circ \tilde{r}$, and $\hat{r}^2 = \tilde{r}^2 = \text{Id}$.

- b) $f \circ s_\sigma = s_\sigma \circ f$, $s_\sigma^2 = \text{Id}$, $\hat{r} \circ s_\sigma = s_\sigma \circ \hat{r}$, and $\tilde{r} \circ s_\sigma = s_\sigma \circ \tilde{r}$.
- c) $f = \hat{r}_\sigma \circ \tilde{r}_\sigma$, and $\hat{r}_\sigma^2 = \tilde{r}_\sigma^2 = \text{Id}$.

Proof.

- a) $\hat{r}(\tilde{r}(q, p)) = \hat{r}(q, \tilde{p}) = \hat{r}(q, -p') = (q', p')$. Besides, $\hat{r}^2(q, p) = \hat{r}(\hat{q}, -p) = (q, p)$, as $Q \cap (\hat{q} + \langle -p \rangle) = \{q, \hat{q}\}$. Finally, $\tilde{r}^2(q, p) = \tilde{r}(q, \tilde{p}) = (q, \tilde{\tilde{p}}) = (q, p)$.
- b) Clearly s_σ is an involution. Since Q is symmetric with regard to the coordinate hyperplanes, it turns out that if p_t and p_n are the tangent and normal components of a velocity p at an impact point q , then σp_t and σp_n are the tangent and normal components of σp at the impact point σq . On the other hand, if we write $q' = q + \mu(q, p')p'$, then $\mu(\sigma q, \sigma p') = \mu(q, p')$, again by the symmetry of Q . Hence, $f \circ s_\sigma = s_\sigma \circ f$. The proof of $\hat{r} \circ s_\sigma = s_\sigma \circ \hat{r}$ and $\tilde{r} \circ s_\sigma = s_\sigma \circ \tilde{r}$ follows the same lines.
- c) It is a direct consequence remark 1. \square

No symmetry has been required to obtain the factorization $f = \hat{r} \circ \tilde{r}$. Therefore, all convex hypersurfaces $Q \subset \mathbb{R}^{n+1}$ give rise to reversible billiard maps, although symmetric hypersurfaces have much more factorizations.

We introduce the acronyms SO, ST, SPO, and SPT for symmetric orbit, symmetric trajectory, symmetric periodic orbit, and symmetric periodic trajectory, respectively. If r is any reversor of the billiard map, we can deal with r -SOs, r -STs, r -SPOs, and r -SPTs.

Once these 2^{n+1} factorizations $f = \hat{r}_\sigma \circ \tilde{r}_\sigma$ have been found, we describe their symmetry sets. In the next proposition we prove that only two symmetry sets are empty. We also provide an explicit geometric description of the $2^{n+2} - 2$ nonempty symmetry sets where one can look for SOs. As a consequence, we shall see that these symmetry sets are mutually exclusive—that is, they do not intersect—but at some very specific points which are described in detail. As before, some notations are required.

We recall that given a reflection defined on an Euclidean space, we can decompose the space as the orthogonal sum of the eigenspaces of eigenvalues -1 and 1 . This is called the *spectral decomposition* of the reflection. Let $\mathbb{R}^{n+1} = V_\sigma^+ \perp V_\sigma^-$ be the spectral decomposition associated to any reflection $\sigma \in \Sigma$. That is,

$$V_\sigma^\pm = \{p \in \mathbb{R}^{n+1} : \sigma p = \pm p\}.$$

For instance, if (x_1, x_2, x_3) are the Cartesian coordinates in \mathbb{R}^3 and $\sigma = \text{diag}(-1, 1, 1)$, then V_σ^+ is the $x_2 x_3$ -plane, and V_σ^- is the x_1 -axis. We also introduce the sections

$$\begin{aligned} Q_\sigma &= Q \cap V_\sigma^+ = \{q \in Q : \sigma q = q\}, \\ P_\sigma &= \mathbb{S}^n \cap V_\sigma^- = \{p \in \mathbb{S}^n : \sigma p = -p\}. \end{aligned}$$

Given two linear varieties $V_1, V_2 \subset \mathbb{R}^{n+1}$, the symbol $V_1 \perp_* V_2$ means that they have a orthogonal intersection. Finally, we recall that a line in \mathbb{R}^{n+1} is a *chord* of Q when it intersects orthogonally Q at two different points.

Proposition 2. *The symmetry sets of the reversors \tilde{r}_σ and \hat{r}_σ , $\sigma \in \Sigma$, are:*

$$\begin{aligned} \text{Fix}(\tilde{r}_\sigma) &= \{(q, p) \in M : q \in Q_\sigma \text{ and } p \in N_q Q_\sigma\}, \\ \text{Fix}(\hat{r}_\sigma) &= \{(q, p) \in M : \sigma q \in q + \langle p \rangle \text{ and } p \in P_\sigma\} \\ &= \{(q, p) \in M : (q + \langle p \rangle) \perp_* V_\sigma^+\}. \end{aligned}$$

Only the reversors $\tilde{r}_{-\text{Id}}$ and \hat{r}_{Id} have empty symmetry sets. Moreover, if a point $(q, p) \in M$ belongs simultaneously to two different symmetry sets, then the line $q + \langle p \rangle$:

- *Is contained in some coordinate hyperplane of \mathbb{R}^{n+1} , in which case so is its whole billiard trajectory; or*
- *Is a chord of the hypersurface Q through the origin, in which case its billiard trajectory is 2-periodic.*

Proof. To begin with, we deduce from the definitions of reversors \tilde{r}_σ and \hat{r}_σ , and symmetries s_σ that

$$\begin{aligned} (q, p) \in \text{Fix}(\tilde{r}_\sigma) &\iff s_\sigma(q, p) = \tilde{r}(q, p) \\ &\iff \left\{ \begin{array}{l} \sigma q = q \\ \sigma p = \tilde{p} \end{array} \right\} \iff \left\{ \begin{array}{l} q \in Q_\sigma \\ \sigma p = \tilde{p} \end{array} \right\}, \\ (q, p) \in \text{Fix}(\hat{r}_\sigma) &\iff s_\sigma(q, p) = \hat{r}(q, p) \\ &\iff \left\{ \begin{array}{l} \sigma q = \hat{q} \\ \sigma p = -p \end{array} \right\} \iff \left\{ \begin{array}{l} \sigma q \in q + \langle p \rangle \\ p \in P_\sigma \end{array} \right\}. \end{aligned}$$

To understand the condition $\sigma p = \tilde{p}$, we compare the spectral decomposition $\mathbb{R}^{n+1} = V_\sigma^+ \perp V_\sigma^-$ with the spectral decomposition $\mathbb{R}^{n+1} \simeq T_q \mathbb{R}^{n+1} = \tilde{V}_q^+ \perp \tilde{V}_q^-$ associated to the reflection $p \mapsto \tilde{p}$. We note that

$$\begin{aligned} \tilde{V}_q^- &= \{p \in T_q \mathbb{R}^{n+1} : \tilde{p} = -p\} = T_q Q, \\ \tilde{V}_q^+ &= \{p \in T_q \mathbb{R}^{n+1} : \tilde{p} = p\} = N_q Q. \end{aligned}$$

If $q \in Q_\sigma$, then

$$\begin{aligned} N_q Q_\sigma &= N_q Q \perp V_\sigma^- = \tilde{V}_q^+ \perp V_\sigma^-, & \tilde{V}_q^+ &\subset V_\sigma^+, \\ T_q Q_\sigma &= T_q Q \cap V_\sigma^+ = \tilde{V}_q^- \cap V_\sigma^+, & V_\sigma^- &\subset \tilde{V}_q^-. \end{aligned}$$

The equality on $N_q Q_\sigma$ is due to $(A \cap B)^\perp = A^\perp \perp B^\perp$. The inclusions follows from V_σ^+ being a symmetry subspace of Q . Those relations imply that

$$\begin{aligned} T_q \mathbb{R}^{n+1} &= N_q Q_\sigma \perp T_q Q_\sigma = \tilde{V}_q^+ \perp V_\sigma^- \perp (\tilde{V}_q^- \cap V_\sigma^+) \\ &= (V_\sigma^+ \cap \tilde{V}_q^+) \perp (V_\sigma^- \cap \tilde{V}_q^-) \perp (\tilde{V}_q^- \cap V_\sigma^+). \end{aligned}$$

Therefore, if we fix any $q \in Q_\sigma$, then $\sigma p = \tilde{p} \iff p \in (V_\sigma^+ \cap \tilde{V}_q^+) \perp (V_\sigma^- \cap \tilde{V}_q^-) = \tilde{V}_q^+ \perp V_\sigma^- = N_q Q_\sigma$, so

$$\text{Fix}(\tilde{r}_\sigma) = \{(q, p) \in M : q \in Q_\sigma, p \in N_q Q_\sigma\}.$$

Next, we study the other symmetry sets for $\sigma \neq \text{Id}$. If $p \in P_\sigma$, then $p \perp V_\sigma^+$ and $p \parallel V_\sigma^-$, which implies that $\sigma q \in q + \langle p \rangle \iff q + \langle p \rangle \perp_* V_\sigma^+$. Therefore,

$$\text{Fix}(\hat{r}_\sigma) = \{(q, p) \in M : q + \langle p \rangle \perp_* V_\sigma^+\}.$$

Clearly, Q_σ is empty if and only if $\sigma = -\text{Id}$, and P_σ is empty if and only if $\sigma = \text{Id}$.

Finally, let us check that if the point $(q, p) \in M$ belongs to two different symmetry sets, then $q + \langle p \rangle$ is a chord of Q or is contained in some coordinate hyperplane like

$$H_j = \{q = (x_1, \dots, x_{n+1}) \in \mathbb{R}^{n+1}; x_j = 0\}. \quad (3)$$

First, if $(q, p) \in \text{Fix}(\tilde{r}_\sigma) \cap \text{Fix}(\tilde{r}_\tau)$, then using the relations written at the beginning of this proof, we get

$$\sigma q = q = \tau q, \quad \sigma p = \tilde{p} = \tau p.$$

If $\sigma \neq \tau$, then $\sigma_j \neq \tau_j$ for some j , so that $q \in H_j$, $p \parallel H_j$, and $q + \langle p \rangle \subset H_j$.

Second, if $(q, p) \in \text{Fix}(\tilde{r}_\sigma) \cap \text{Fix}(\hat{r}_\tau)$, then using again the same relations, we get that

$$\sigma q = q, \quad \sigma p = \tilde{p} = -p', \quad \tau q = \hat{q}, \quad \tau p = -p.$$

If $\sigma \neq \text{Id}$, then $\sigma_j = -1$ for some j , so that $q, \hat{q} \in H_j$, $p \parallel H_j$, and $q + \langle p \rangle \subset H_j$. If $\sigma = \text{Id}$ but $\tau \neq -\text{Id}$, then $\tau_j = 1$ for some j , so that $p' = -p \in N_q Q$, $p \parallel H_j$, and $p' \parallel H_j$. Thus, $p_n \parallel H_j$ and $N_q Q \subset H_j$, which implies that $q \in H_j$, because Q is symmetric, smooth, and (strictly) convex. Therefore, $q + \langle p \rangle \subset H_j$. If $\sigma = \text{Id}$ and $\tau = -\text{Id}$, then $p' = -p \in N_q Q$ and $\hat{q} = -q$, so that the line $q + \langle p \rangle$ intersects orthogonally Q at q and $-q$.

Third, if $(q, p) \in \text{Fix}(\hat{r}_\sigma) \cap \text{Fix}(\hat{r}_\tau)$, then

$$\sigma q = \hat{q} = \tau q, \quad \sigma p = -p = \tau p,$$

and we apply the same reasoning as in the first case. \square

Hence, only very specific billiard orbits —the ones contained in a coordinate hyperplane or 2-periodic— can have a point in the intersection of two symmetry sets. For instance, it turns out that any 2-periodic billiard orbit inside a nondegenerate ellipsoid is contained in more than half of the $2^{n+2} - 2$ nonempty symmetry sets.

Nevertheless, there exists other billiard orbits that intersect different symmetry sets, but at different points. Indeed, all SPOs with odd period have points on two associated symmetry sets, whereas all SPOs with even period have *two* points on some symmetry set; see item c) of Theorem 1. However, a especial situation arises when Q is an ellipsoid: most of its SPOs with even period have exactly *four* —instead of the expected two— points in the symmetry sets described in Proposition 2, in which case they must intersect two different symmetry sets (see item b) of Theorem 1).

That motivates the following definition.

Definition 7. An SPO inside a symmetric hypersurface $Q \subset \mathbb{R}^{n+1}$, is a doubly SPO when it intersects two different symmetry sets.

Remark 2. Let O be a \tilde{r}_σ -SO or, equivalently, a \hat{r}_σ -SO (see Theorem 1). By definition, O , as a subset of the phase space M , is invariant under the reversors

$$\tilde{r}_\sigma(q, p) = (\sigma q, \sigma \tilde{p}), \quad \hat{r}_\sigma(q, p) = (\sigma \hat{q}, -\sigma p).$$

In particular, the billiard configuration associated to O , viewed as a subset of the configuration space Q , is invariant under the map $\sigma|_Q: q \mapsto \sigma q$, whereas its velocity configuration, viewed as a subset of the velocity space \mathbb{S}^n , is invariant under the map $-\sigma|_{\mathbb{S}^n}: p \mapsto -\sigma p$. This motivates the following definitions for the 2D and 3D cases. A billiard configuration inside a symmetric curve/surface is called *central*, *axial* or *specular* when it is symmetric with regard to the origin, some axis of coordinates or some plane of coordinates, respectively. Similar definitions apply to velocity configurations.

4 Billiards inside ellipsoids of \mathbb{R}^{n+1}

The billiard dynamics inside ellipsoids has several important properties. For instance, it is completely integrable in the sense of Liouville. We present some results about such billiards. First, we list the classical ones, which can be found in the monographs [23, 28, 29]. Next, we describe a useful symmetry contained in [9, 30]. Finally, we detail the behaviour of elliptic coordinates of billiard trajectories inside ellipsoids given in [13].

4.1 Caustics and elliptic coordinates

The following results go back to Jacobi, Chasles, Poncelet, and Darboux. We consider a billiard inside the ellipsoid

$$Q = \{q \in \mathbb{R}^{n+1}; \langle Dq, q \rangle = 1\}, \quad (4)$$

where $D^{-1} = \text{diag}(a_1, \dots, a_{n+1})$ is a diagonal matrix such that $0 < a_1 < \dots < a_{n+1}$. The degenerate cases in which the ellipsoid has some symmetry of revolution are not considered here. This ellipsoid is an element of the family of confocal quadrics given by

$$Q_\mu = \{q \in \mathbb{R}^{n+1}; \langle D_\mu q, q \rangle = 1\}, \quad \mu \in \mathbb{R},$$

where $D_\mu = (D^{-1} - \mu \text{Id})^{-1}$. The meaning of Q_μ in the singular cases $\mu \in \{a_1, \dots, a_{n+1}\}$ must be clarified. If $\mu = a_j$, then we define it as the n -dimensional hyperplane (3).

Theorem 2. Let Q be the nondegenerate ellipsoid (4).

- Any generic point $q \in \mathbb{R}^{n+1}$ belongs to exactly $n + 1$ distinct nonsingular quadrics $Q_{\mu_0}, \dots, Q_{\mu_n}$ such that $\mu_0 < a_1 < \mu_1 < a_2 < \dots < a_n < \mu_n < a_{n+1}$. Besides, those $n + 1$ quadrics are mutually orthogonal at q .
- Any generic line $\ell \subset \mathbb{R}^{n+1}$ is tangent to exactly n distinct nonsingular confocal quadrics $Q_{\lambda_1}, \dots, Q_{\lambda_n}$ such that $\lambda_1 < \dots < \lambda_n$, $\lambda_1 \in (-\infty, a_1) \cup (a_1, a_2)$, and $\lambda_i \in (a_{i-1}, a_i) \cup (a_i, a_{i+1})$, for $i = 2, \dots, n$.

Set $a_0 = 0$. If a generic point q is in the interior of the ellipsoid Q , then $\mu_1 > 0$, so $a_0 < \mu_0 < a_1$. In the same way, if a generic line ℓ has a transverse intersection with the ellipsoid Q , then $\lambda_1 > 0$, so $\lambda_1 \in (a_0, a_1) \cup (a_1, a_2)$. The values $\mu_0 = 0$ and $\lambda_1 = 0$ are attained just when $q \in Q$ and ℓ is tangent to Q , respectively.

We denote by $\mathbf{q} = (\mu_0, \dots, \mu_n) \in \mathbb{R}^{n+1}$, the *Jacobi elliptic coordinates* of the point $q = (x_1, \dots, x_{n+1})$. Cartesian and elliptic coordinates are linked by relations

$$x_j^2 = \frac{\prod_{i=0}^n (a_j - \mu_i)}{\prod_{i \neq j} (a_j - a_i)}, \quad j = 1, \dots, n+1. \quad (5)$$

Elliptic coordinates define a coordinate system on each of the 2^{n+1} open orthants of the Euclidean space \mathbb{R}^{n+1} , but they become singular at the $n+1$ coordinate hyperplanes, because the map $q \mapsto \mathbf{q}$ is not one-to-one in any neighborhood of these hyperplanes.

A point is *generic*, in the sense of Theorem 2, if and only if it is outside all coordinate hyperplanes. From (5), we deduce that when the point q tends to the hyperplane H_j , some elliptic coordinate μ_i tends to a_j . In fact, $i = j$ or $i = j - 1$, because of the inequalities $a_i < \mu_i < a_{i+1}$.

A line is *generic*, in the sense of Theorem 2, if and only if it is neither tangent to a singular confocal quadric nor contained in a nonsingular confocal quadric.

If two lines obey the reflection law at a point $q \in Q$, then both lines are tangent to the same confocal quadrics. This shows a tight relation between elliptic billiards and confocal quadrics: all lines of a billiard trajectory inside the ellipsoid Q are tangent to exactly n confocal quadrics $Q_{\lambda_1}, \dots, Q_{\lambda_n}$, which are called *caustics* of the trajectory. We will say that $\lambda = (\lambda_1, \dots, \lambda_n) \in \mathbb{R}^n$ is the *caustic parameter* of the trajectory.

Definition 8. A billiard trajectory inside a nondegenerate ellipsoid Q is nonsingular when it has n distinct nonsingular caustics; that is, when its caustic parameter belongs to the nonsingular caustic space

$$\Lambda = \{\lambda \in \mathbb{R}^n : 0 < \lambda_1 < \dots < \lambda_n, \lambda_i \in (a_{i-1}, a_i) \cup (a_i, a_{i+1})\}.$$

We will only deal with nonsingular billiard trajectories along this paper.

Remark 3. The set Λ has 2^n connected components, being each one associated to a different type of caustics. For instance, in the 2D case ($n = 1$) the two connected components correspond to ellipses and hyperbolas.

Theorem 3. If a nonsingular billiard trajectory closes after l bounces, all trajectories sharing the same caustics also close after l bounces.

Poncelet and Darboux proved this theorem for ellipses and triaxial ellipsoids of \mathbb{R}^3 , respectively. Later on, it was generalized to any dimension in [9].

4.2 A dual symmetry

Since the ellipsoid (4) is symmetric with regard to all coordinate hyperplanes, its billiard map has the 2^{n+1} symmetries s_σ . Here, we present a new symmetry g that takes place only for billiards inside ellipsoids. It exchanges the role of positions and velocities—so, it could be seen as a dual symmetry—and was introduced in [9, 30]. The following explicit formulae are required to define g .

Proposition 3. The billiard map $f: M \rightarrow M$ inside the ellipsoid (4) is expressed by $f(q, p) = (q', p')$, where

$$\begin{cases} q' = q + \mu(q, p')p', & \mu(q, p') = -2 \frac{\langle Dq, p' \rangle}{\langle Dp', p' \rangle}, \\ p' = p + \nu(q, p)Dq, & \nu(q, p) = -2 \frac{\langle Dq, p \rangle}{\langle Dq, Dq \rangle}. \end{cases}$$

Besides, the reversors $\hat{r}, \tilde{r}: M \rightarrow M$ are given by:

$$\begin{cases} \hat{r}(q, p) = (\hat{q}, -p), & \hat{q} = q + \mu(q, p)p, \\ \tilde{r}(q, p) = (q, \tilde{p}), & \tilde{p} = -p - \nu(q, p)Dq. \end{cases}$$

Proof. The formulae for the billiard map are well known. See, for instance, [30]. Next, to obtain the formula for \hat{r} we recall that \hat{q} is the previous impact point, so

$$\hat{q} = q + \mu(q, -p)(-p) = q + \mu(q, p)p.$$

Finally, the formula for \tilde{r} follows from $\tilde{p} = -p'$. \square

We are ready to introduce the dual symmetry g . We check that, in certain sense, g is the square root of the billiard map f . In particular, g has the same symmetries and reversors as f . From our point of view, its most useful property is that it interchanges some symmetry sets.

Proposition 4. Let $g: M \rightarrow M$, $g(q, p) = (\bar{q}, \bar{p})$, where:

$$\begin{cases} \bar{q} = Cp' = Cp + \nu(q, p)C^{-1}q, \\ \bar{p} = -C^{-1}q, \end{cases}$$

with $C = D^{-1/2}$. Then the following relations are fulfilled:

- $g^2 = -f$, and $f \circ g = g \circ f$.
- $g \circ s_\sigma = s_\sigma \circ g$ for all $\sigma \in \Sigma$.
- $\hat{r} \circ g = -g \circ \tilde{r}$, $g \circ \tilde{r} \circ g = \tilde{r}$, and $g \circ \hat{r} \circ g = \hat{r}$.
- $g(\text{Fix}(\tilde{r}_\sigma)) = \text{Fix}(\hat{r}_{-\sigma}) = \text{Fix}(f \circ \tilde{r}_{-\sigma})$ for all $\sigma \in \Sigma$.

Proof.

- We observe two relations:

$$\begin{aligned} \nu(\bar{q}, \bar{p}) &= -2 \frac{\langle D\bar{q}, \bar{p} \rangle}{\langle D\bar{q}, D\bar{q} \rangle} = 2 \frac{\langle Dq, p' \rangle}{\langle Dp', p' \rangle} \\ &= -\mu(q, p') = \mu(q, \tilde{p}), \\ \mu(\bar{q}, \bar{p}) &= -2 \frac{\langle D\bar{q}, \bar{p} \rangle}{\langle D\bar{p}, \bar{p} \rangle} = 2 \frac{\langle Dq, p' \rangle}{\langle Dq, Dq \rangle} \\ &= -\nu(q, p') = \nu(q, \tilde{p}). \end{aligned}$$

Thus $\nu \circ g = \mu \circ \tilde{r}$ and $\mu \circ g = \nu \circ \tilde{r}$, and then $g^2 = -f$:

$$\begin{aligned} g^2(q, p) &= g(\bar{q}, \bar{p}) = (C\bar{p} + \nu(\bar{q}, \bar{p})C^{-1}\bar{q}, -C^{-1}\bar{q}) \\ &= (-q - \mu(q, p')p', -p') = (-q', -p'). \end{aligned}$$

It is immediate that g is odd. Therefore,

$$f \circ g = (-g^2) \circ g = -g^3 = g \circ (-g^2) = g \circ f.$$

- It is obvious.

- By using a) and definition of g :

$$\begin{aligned} g(q, \tilde{p}) &= (C\tilde{p} + \nu(q, \tilde{p})C^{-1}q, -C^{-1}q) \\ &= (-\bar{q} - \mu(\bar{q}, \bar{p})\bar{p}, \bar{p}) = -\hat{r}(\bar{q}, \bar{p}). \end{aligned}$$

As a consequence $\hat{r} \circ g = -g \circ \tilde{r}$ and besides:

$$\begin{aligned}\hat{r} &= f \circ \tilde{r} = -g^2 \circ \tilde{r} = g \circ \hat{r} \circ g, \\ \tilde{r} &= f \circ \tilde{r} \circ f = \hat{r} \circ f = \hat{r} \circ (-g^2) \\ &= -\hat{r} \circ g^2 = g \circ \tilde{r} \circ g.\end{aligned}$$

d) Because g is a diffeomorphism we have that:

$$\begin{aligned}m \in \text{Fix}(\tilde{r}_\sigma) &\iff g(m) = g(\tilde{r}_\sigma(m)) = -\hat{r}_\sigma(g(m)) \\ &\iff g(m) \in \text{Fix}(\hat{r}_{-\sigma}).\end{aligned}$$

We have used that $-\hat{r}_\sigma = \hat{r}_{-\sigma}$. Consequently,

$$g(\text{Fix}(\tilde{r}_\sigma)) = \text{Fix}(\hat{r}_{-\sigma}) = \text{Fix}(f \circ \tilde{r}_{-\sigma}). \quad \square$$

The last item of this proposition has a practical corollary.

Corollary 1. *The dual symmetry $g: M \rightarrow M$ gives an explicit one-to-one correspondence between \tilde{r}_σ -SPOs and $(f \circ \tilde{r}_{-\sigma})$ -SPOs of the same period.*

Proof. Let $m \in \text{Fix}(\tilde{r}_\sigma)$ be a point of the phase space such that its orbit O , is l -periodic. Thus, O is a \tilde{r}_σ -SPO. Let us consider the orbit \bar{O} by the point $\bar{m} = g(m)$. First,

$$f^l(\bar{m}) = f^l(g(m)) = g(f^l(m)) = g(m) = \bar{m}.$$

Thus, \bar{O} is l -periodic. Second, $\bar{m} = g(m) \in \text{Fix}(\hat{r}_{-\sigma})$, so \bar{O} is a $\hat{r}_{-\sigma}$ -SPO. Therefore, we have explicitly constructed the correspondence $g: O \mapsto \bar{O}$, which is one-to-one since $g^2 = -f$. \square

In subsequent sections we carry out some computations on SPOs only for reversors $\{\tilde{r}_\sigma: \sigma \in \Sigma\}$, since from this corollary, we deduce the analogous results for reversors $\{\hat{r}_\sigma = f \circ \tilde{r}_\sigma: \sigma \in \Sigma\}$.

4.3 Elliptic coordinates of SPTs

The behaviour of elliptic coordinates along nonsingular billiard trajectories inside a nondegenerate ellipsoid, can be summarized as follows. If a particle obeys the billiard dynamics, describing a polygonal curve of \mathbb{R}^{n+1} whose vertexes are on the ellipsoid, then its i -th elliptic coordinate μ_i oscillates inside some interval $I_i = [c_{2i}, c_{2i+1}]$ in such a way that its only critical points are attained when $\mu_i \in \partial I_i$. In other words, the oscillation has amplitude $c_{2i+1} - c_{2i}$. This is a classical result that can be found, for instance, in [13]. Let us state it as a formal theorem.

In order to describe the intervals I_i , we set

$$\{c_1, \dots, c_{2n+1}\} = \{a_1, \dots, a_{n+1}\} \cup \{\lambda_1, \dots, \lambda_n\},$$

once ellipsoid parameters a_1, \dots, a_{n+1} , and caustic parameters $\lambda_1, \dots, \lambda_n$, are fixed.

If $\lambda \in \Lambda$, then c_1, \dots, c_{2n+1} are pairwise distinct and positive, so we can assume that

$$c_0 := 0 < c_1 < \dots < c_{2n+1}.$$

Then $I_i = [c_{2i}, c_{2i+1}]$, $0 \leq i \leq n$, are the intervals that we were looking for.

Theorem 4. *Let $q(t)$ be an arc-length parameterization of a nonsingular billiard trajectory inside the ellipsoid (4), sharing caustics $Q_{\lambda_1}, \dots, Q_{\lambda_n}$. Let $\mathbf{q}(t) = (\mu_0(t), \dots, \mu_n(t))$ be the corresponding parameterization in elliptic coordinates. The following properties are satisfied:*

a) $c_{2i} \leq \mu_i(t) \leq c_{2i+1}$ for all $t \in \mathbb{R}$.

b) Functions $\mu_i(t)$ are smooth everywhere, except $\mu_0(t)$ which is nonsmooth at impact points —that is, when $q(t_*) \in Q-$, in which case $\mu'_0(t_*+) = -\mu'_0(t_*-) \neq 0$.

c) If $\mu_i(t)$ is smooth at $t = t_*$, then

$$\mu'_i(t_*) = 0 \iff \mu_i(t_*) \in \{c_{2i}, c_{2i+1}\}.$$

d) If the trajectory is periodic with length L_0 , then $\mathbf{q}(t)$ is L_0 -periodic and there exist some positive integers m_0, \dots, m_n , called winding numbers, such that $\mu_i(t)$ makes exactly m_i complete oscillations (round trips) inside the interval $I_i = [c_{2i}, c_{2i+1}]$ along one period $0 \leq t \leq L_0$. Besides,

i. m_0 is the period of the billiard trajectory.

ii. m_i is even when $\{c_{2i}, c_{2i+1}\} \cap \{a_1, \dots, a_{n+1}\} \neq \emptyset$.

iii. $\mathbf{q}(t)$ has period $L_0/2$ if and only if all winding numbers are even, but it never has period $L_0/4$.

iv. Not all winding numbers can be multiples of four.

Thus, all billiard trajectories sharing caustics $Q_{\lambda_1}, \dots, Q_{\lambda_n}$ are contained in the $(n+1)$ -dimensional cuboid

$$C_\lambda := I_0 \times \dots \times I_n = [0, c_1] \times \dots \times [c_{2n}, c_{2n+1}] \subset \mathbb{R}^{n+1},$$

when they are expressed in elliptic coordinates. Besides, a billiard trajectory drawn in elliptic coordinates, has elastic reflections with the n -dimensional face $\{\mu_0 = 0\}$, of the cuboid, but inner tangent contacts with the other $2n+1$ faces. This behaviour can be observed in Table 6, where several SPTs are drawn in Cartesian and elliptic coordinates. The cuboid is just a rectangle in those cases.

Based on extensive numerical experiments, it has been conjectured that

$$2 \leq m_n < \dots < m_1 < m_0, \quad (6)$$

but we are not aware of any proof. See [5] for details.

5 2D case

5.1 Caustics and elliptic coordinates

We adapt the previous setting of billiards inside ellipsoids of \mathbb{R}^{n+1} to the 2D case; that is, $n = 1$. Then the configuration space is an ellipse Q , which, in order to simplify the exposition, we write as

$$Q = \left\{ q = (x, y) \in \mathbb{R}^2: \frac{x^2}{a} + \frac{y^2}{b} = 1 \right\}, \quad a > b > 0.$$

As we said in Subsec. 4.1, any nonsingular billiard trajectory inside Q is tangent to one confocal caustic

$$Q_\lambda = \left\{ q = (x, y) \in \mathbb{R}^2: \frac{x^2}{a-\lambda} + \frac{y^2}{b-\lambda} = 1 \right\},$$

where the caustic parameter λ belongs to the nonsingular caustic space

$$\Lambda = E \cup H, \quad E = (0, b), \quad H = (b, a).$$

The names of the connected components of Λ come from the fact that Q_λ is an confocal ellipse for $\lambda \in E$ and a confocal hyperbola for $\lambda \in H$. The singular cases $\lambda = b$ and $\lambda = a$ correspond to the x -axis and y -axis, respectively. We say that the *caustic type* of a billiard trajectory is E or H, when its caustic is an ellipse or a hyperbola. We also distinguish between E-caustics and H-caustics.

We denote by $q = (e, h)$ the Jacobi elliptic coordinates of the point $q = (x, y)$. That is, q belongs to the orthogonal intersection of the confocal ellipse Q_e and the confocal hyperbola Q_h . We recall from (5) that

$$x^2 = \frac{(a-e)(a-h)}{a-b}, \quad y^2 = \frac{(b-e)(h-b)}{a-b}.$$

Besides, $0 < e < b < h < a$ if the point q is contained in the interior of Q , and $e = 0$ at impact points $q \in Q$. The y -axis is $\{h = a\}$, the x -axis is $\{e = b\} \cup \{h = b\}$, and the foci of the ellipse verify $e = h = b$, in elliptic coordinates. Likewise, the four points $(\pm x, \pm y)$ have associated the same elliptic coordinates (e, h) , so this system of coordinates do not distinguish among the four quadrants in \mathbb{R}^2 .

We also know that all billiard trajectories sharing the caustic Q_λ are contained in the rectangle

$$\mathcal{C}_\lambda = [0, \min(b, \lambda)] \times [\max(b, \lambda), a] \subset \mathbb{R}^2 \quad (7)$$

when they are expressed in terms of (e, h) . Moreover, the coordinates e and h have a monotone behaviour except at the endpoints of the intervals that enclose them. The geometric meaning of the sides and vertexes of the rectangle \mathcal{C}_λ is described in Fig. 2. In the figure, black, red and gray sides means impact with the ellipse Q , tangency with the caustic Q_λ , and crossing some coordinate axis, respectively. This color code is repeated in Table 5.

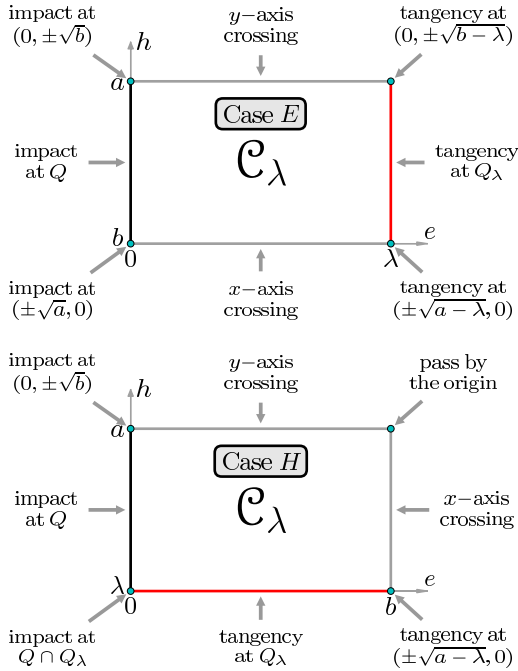


Figure 2. Geometric meaning of sides and vertexes of \mathcal{C}_λ .

5.2 Rotation number and winding numbers

We recall some concepts related to periodic trajectories of billiards inside ellipses. These results can be found, for instance, in [5, 9].

To begin with, we introduce the function $\rho: \Lambda \rightarrow \mathbb{R}$ given by the quotient of elliptic integrals

$$\rho(\lambda) = \frac{\int_0^{\min(b, \lambda)} \frac{ds}{\sqrt{(\lambda-s)(b-s)(a-s)}}}{2 \int_{\max(b, \lambda)}^a \frac{ds}{\sqrt{(\lambda-s)(b-s)(a-s)}}}.$$

This function is called the *rotation number*. It allows us to characterize the caustic parameters that give rise to periodic trajectories. To be precise, the billiard trajectories sharing the caustic Q_λ are periodic if and only if

$$\rho(\lambda) = m_1/2m_0 \in \mathbb{Q}$$

for some integers $2 \leq m_1 < m_0$, which are the *winding numbers*. It turns out that m_0 is the period, $m_1/2$ is the number of turns around the ellipse Q_λ for E-caustics, and m_1 is the number of crossings of the y -axis for H-caustics. Thus, m_1 is always even. Besides, all periodic trajectories with H-caustics have even period.

5.3 Reversors and their symmetry sets

We also change the notations for reversors. We denote by R the reversor previously written as \tilde{r} . Besides, R_x , R_y , and R_{xy} are the reversors obtained by composing R with the symmetries defined on the phase space and associated to the reflections $(x, y) \mapsto (-x, y)$, $(x, y) \mapsto (x, -y)$, and $(x, y) \mapsto (-x, -y)$, respectively. Finally, $f \circ R$, $f \circ R_x$, $f \circ R_y$, and $f \circ R_{xy}$ denote the four reversors of the form $\{\hat{r}_\sigma = f \circ \tilde{r}_\sigma: \sigma \in \Sigma\}$. We proved in Proposition 2 that the symmetry sets of R_{xy} and $f \circ R$ are empty sets, and following the same proposition we get:

- $\text{Fix}(R) = \{(q, p) \in M: p \in N_q Q\}$,
- $\text{Fix}(R_x) = \{(q, p) \in M: q = (0, \pm\sqrt{b})\}$,
- $\text{Fix}(R_y) = \{(q, p) \in M: q = (\pm\sqrt{a}, 0)\}$,
- $\text{Fix}(f \circ R_x) = \{(q, p) \in M: p = (\pm 1, 0)\}$,
- $\text{Fix}(f \circ R_y) = \{(q, p) \in M: p = (0, \pm 1)\}$, and
- $\text{Fix}(f \circ R_{xy}) = \{(q, p) \in M: 0 \in q + \langle p \rangle\}$.

Here, $M = \{(q, p) \in Q \times \mathbb{S}: p \text{ is directed outward } Q \text{ at } q\}$ is the phase space. We write $q = (x, y)$ and $p = (u, v)$.

5.4 Characterization of STs

In order to find caustics Q_λ , whose tangent trajectories are periodic, we solve equation $\rho(\lambda) = m_1/2m_0$, for some winding numbers $2 \leq m_1 < m_0$. Hence, once we fix a caustic parameter λ such that $\rho(\lambda) = m_1/2m_0 \in \mathbb{Q}$, and a reversor $r: M \rightarrow M$, it is natural to look for points $(q, p) \in \text{Fix}(r)$ such that $q + \langle p \rangle$ is tangent to Q_λ . If we can find those points, billiard trajectories associated to them are r -SPTs of period m_0 .

In the 2D case there are only $6(=2^3 - 2)$ nonempty symmetry sets where one can look for STs; see previous subsection. We write the six formulae for (q, p) in Table 2. The cases where p is directed inward Q at q are excluded from this table, because we require $(q, p) \in M$.

r	$q = (x, y), p = (u, v)$
R	$x^2 = \frac{a(a-\lambda)}{a-b}, y^2 = \frac{b(\lambda-b)}{a-b},$ $p = \mu(x/a, y/b), \mu = \sqrt{ab/\lambda}$
R_x	$q = (0, \pm\sqrt{b}), u^2 = \frac{a-\lambda}{a}, v^2 = \frac{\lambda}{a}$
R_y	$q = (\pm\sqrt{a}, 0), u^2 = \frac{\lambda}{b}, v^2 = \frac{b-\lambda}{b}$
$f \circ R_x$	$x^2 = \frac{a\lambda}{b}, y^2 = b - \lambda, p = (\pm 1, 0)$
$f \circ R_y$	$x^2 = a - \lambda, y^2 = \frac{b\lambda}{a}, p = (0, \pm 1)$
$f \circ R_{xy}$	$u^2 = \frac{a-\lambda}{a-b}, v^2 = \frac{\lambda-b}{a-b}, q = \sqrt{ab/\lambda} p$

Table 1. Points $(q, p) \in \text{Fix}(r)$ such that $q + \langle p \rangle$ is tangent to Q_λ .

Let us check the first 3 cases in Table 1. The formulae for $f \circ R_x, f \circ R_y$ and $f \circ R_{xy}$ follow from their dual reversors R_y, R_x and R , respectively. See Corollary 1. Suffice it to perform the changes $u^2 \leftrightarrow x^2/a$ and $v^2 \leftrightarrow y^2/b$ in the first formulae. This has to do with the fact that the dual symmetry $g: M \rightarrow M, g(q, p) = (\bar{q}, \bar{p}), \bar{p} = (\bar{u}, \bar{v})$ verifies that $\bar{u} = -x/\sqrt{a}$ and $\bar{v} = -y/\sqrt{b}$.

R . We look for $(q, p) \in M$ such that $p \in N_q Q$ and $q + \langle p \rangle$ is tangent to Q_λ . If $p \in N_q Q$, then there exists $\mu > 0$ such that $p = \mu(x/a, y/b)$. If, in addition, $q + \langle p \rangle$ is tangent to Q_λ , then Q_λ is a hyperbola and $q \in Q \cap Q_\lambda$. Here, we have used that confocal ellipses and confocal hyperbolas are mutually orthogonal. Thus, the elliptic coordinates of $q = (x, y)$ are $(e, h) = (0, \lambda)$, and so $x^2 = a(a-\lambda)/(a-b)$ and $y^2 = b(\lambda-b)/(a-b)$. Finally, we recall that p is a unit velocity:

$$1 = u^2 + v^2 = \mu^2 \left(\frac{x^2}{a^2} + \frac{y^2}{b^2} \right) = \frac{\lambda \mu^2}{ab} \implies \mu^2 = \frac{ab}{\lambda}.$$

R_x . We look for a velocity $p = (u, v) \in \mathbb{S}$ such that $q + \langle p \rangle$ has exactly one point on Q_λ for $q = (0, \pm\sqrt{b})$. This condition turns into the uniqueness of solutions in t of

$$\alpha t^2 + 2\beta t + \gamma = 0,$$

where

$$\alpha = \frac{u^2}{a-\lambda} + \frac{v^2}{b-\lambda}, \quad \beta = \frac{\pm\sqrt{b}v}{b-\lambda}, \quad \gamma = \frac{\lambda}{b-\lambda},$$

or equivalently $\beta^2 = \alpha\gamma$. This last equality together with $u^2 + v^2 = 1$ gives $v^2 = \lambda/a$ and $u^2 = (a-\lambda)/a$.

R_y . It is obtained directly from the previous case by exchanging the role of coordinates x and y .

Next, we characterize nonsingular STs inside noncircular ellipses, as the trajectories passing, in elliptic coordinates, through some vertex of the rectangle \mathcal{C}_λ .

We only have to check that any vertex $q_* \in \mathcal{C}_\lambda$, corresponds to some point $q_* \in q + \langle p \rangle$, such that $q + \langle p \rangle$ is tangent to Q_λ and $(q, p) \in \text{Fix}(r)$ for some reversor r . We list such correspondences in Table 2. The point q_* is not unique, because elliptic coordinates do not distinguish among the four quadrants in \mathbb{R}^2 . In its last column we describe the feasible reversors for each caustic type; see Subsec. 5.5 for more detailed information.

Vertex (e, h)	q_* belongs to	Reversor	Type
$(0, \lambda)$	$Q \cap Q_\lambda$	R	H
$(0, a)$	$Q \cap \{y\text{-axis}\}$	R_x	any
$(0, b)$	$Q \cap \{x\text{-axis}\}$	R_y	E
(λ, a)	$Q_\lambda \cap \{y\text{-axis}\}$	$f \circ R_x$	E
(λ, b) or (b, λ)	$Q_\lambda \cap \{x\text{-axis}\}$	$f \circ R_y$	any
(b, a)	$\{(0, 0)\}$	$f \circ R_{xy}$	H

Table 2. Points in STs that correspond to vertexes of \mathcal{C}_λ .

For instance, let us focus on the vertex $q_* = (0, \lambda)$. It is a vertex of \mathcal{C}_λ if and only if $b < \lambda < a$, so the type of caustic is H. We note that $q_* \in Q$ since $e = 0$, and $q_* \in Q_\lambda$ since $h = \lambda$. Let $p \in \mathbb{S}$ be the unique outward velocity such that $q_* + \langle p \rangle$ is tangent to Q_λ . Then $p \in N_{q_*} Q$, since the confocal hyperbola Q_λ has a orthogonal intersection at q_* with the ellipse Q . Hence, $(q_*, p) \in \text{Fix}(R)$. The other cases are similar. We only observe that $e \neq 0$ in the last three cases, so $q_* \notin Q$; but q_* is the middle point of two consecutive impact points.

5.5 Forbidden reversors for each type of caustic

Although there are 6 nonempty symmetry sets, once the caustic type (E or H) is fixed, only 4 of them give rise to SPTs of that type. The correspondences between caustic types and reversors whose symmetry sets are feasible or forbidden are listed in Table 3.

Type	Feasible	Forbidden
E	$R_x, R_y, f \circ R_x, f \circ R_y$	$R, f \circ R_{xy}$
H	$R, R_x, f \circ R_y, f \circ R_{xy}$	$R_y, f \circ R_x$

Table 3. Feasible and forbidden reversors for each caustic type.

To check that all couples caustic type/feasible reversor take really place, we show some examples in Table 5.

We can prove Table 3 in three different ways. Firstly, by means of analytical arguments based on the formulae listed in Table 1. Secondly, we could deduce it by using elliptic coordinates, as shown in Table 2. Finally, we could write a geometric proof. The first way is the simplest one. If $(q, p) \in \text{Fix}(R)$, then $y^2 = b(\lambda-b)/(a-b)$, so $\lambda > b$ and Q_λ is a hyperbola. If $(q, p) \in \text{Fix}(R_{xy})$, then $v^2 = (\lambda-b)/(a-b)$, so $\lambda > b$ and Q_λ is a hyperbola. If $(q, p) \in \text{Fix}(R_y)$, then $v^2 = (b-\lambda)/b$, so $\lambda < b$ and Q_λ is an ellipse. If $(q, p) \in \text{Fix}(f \circ R_x)$, then $y^2 = b - \lambda$, so $\lambda < b$ and Q_λ is an ellipse. This ends the proof.

5.6 Characterization and classification of SPTs

Next, we give a complete classification of nonsingular SPTs inside noncircular ellipses. We classify them by caustic type (E or H) and symmetry sets they meet. We also characterize them as trajectories connecting, in elliptic coordinates, two vertexes of the rectangle \mathcal{C}_λ .

Along this subsection, O denotes a r -SO through a point $(q, p) \in \text{Fix}(r)$, for some reversor $r: M \rightarrow M$. We set $(q_j, p_j) = f^j(q, p)$, $q_j = (x_j, y_j)$, and $p_j = (u_j, v_j)$, for $j \in \mathbb{Z}$. The properties listed in Table 4 are easily deduced using geometric arguments from the symmetry of the ellipse.

r	Properties
R	$q_{-j} = q_j, p_{-j+1} = -p_j$
R_x	$q_{-j} = (-x_j, y_j), p_{-j} = (u_{j+1}, -v_{j+1})$
R_y	$q_{-j} = (x_j, -y_j), p_{-j} = (-u_{j+1}, v_{j+1})$
$f \circ R_x$	$q_{-(j+1)} = (-x_j, y_j), p_{-j} = (u_j, -v_j)$
$f \circ R_y$	$q_{-(j+1)} = (x_j, -y_j), p_{-j} = (-u_j, v_j)$
$f \circ R_{xy}$	$q_{-(j+1)} = -q_j, p_{-j} = p_j$

Table 4. Properties of $(q_j, p_j) = f^j(q, p)$ when $(q, p) \in \text{Fix}(r)$.

For instance, let us explain the case of reversor R_y . If $(q, p) \in \text{Fix}(R_y)$, then $x_0 = \pm\sqrt{a}$ and $y_0 = 0$. Let us assume that $x_0 = \sqrt{a}$. Then it is geometrically evident that $q_{-j} = (x_j, -y_j)$ and the billiard configuration is symmetric with regard to the x -axis; see Fig. 3.

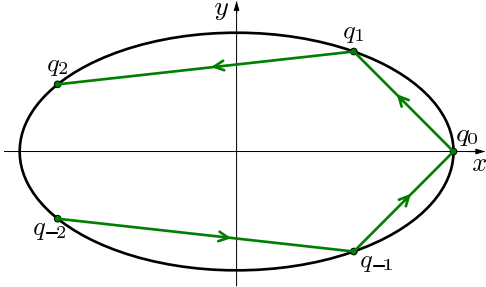


Figure 3. A R_y -ST.

We note that all properties concerning velocities p_j can be directly deduced from the properties of impact points q_j , by using identity (2).

Below, we suppose O is periodic as well, with winding numbers $2 \leq m_1 < m_0$, m_0 being its period. We need a technical lemma on SPOs of even period.

Lemma 2. *Let us assume that the period is even: $m_0 = 2l$, and the reversor is $r = R_x$, so that $x_0 = 0$.*

a) *If the caustic is an ellipse, then $q_l = -q_0$ and $p_l = -p_0$. As a consequence, $q_{l+j} = -q_j$ and $p_{l+j} = -p_j, \forall j \in \mathbb{Z}$.*

b) *If the caustic is a hyperbola, then $q_l = (-1)^l q_0$ and*

$$p_l = \begin{cases} (u_0, -v_0), & \text{if } l \text{ odd and } m_1/2 \text{ even,} \\ (-u_0, v_0), & \text{if } l \text{ even,} \\ (-u_0, -v_0), & \text{if } l \text{ odd and } m_1/2 \text{ odd.} \end{cases}$$

Proof. The hypothesis $r = R_x$ in a), implies $x_{-j} = -x_j$; see Table 5. Then, as $m_0 = 2l$, we have $x_l = x_{-l} = -x_l$, so $x_l = 0$ and $q_l \in \{q_0, -q_0\}$. If $q_l = q_0$, then $p_l = p_0$, since the line $q_l + \langle p_l \rangle$ must be tangent to the ellipse Q_λ and the billiard trajectory turns around Q_λ in a constant—clockwise or anticlockwise—direction. But the period cannot be smaller than m_0 by hypothesis. Hence, $q_l = -q_0$. Finally, the identity $p_l = -p_0$ is necessary to keep the rotation direction around Q_λ . The formulae for a general integer j are obvious.

We skip the proof for H-caustics in b): it is similar. \square

Following we prove that all SPOs inside a noncircular ellipse are doubly SPOs and that there are 12 classes of SPOs, as claimed in the introduction. We recall that SPOs are classified by caustic type and met symmetry sets.

Theorem 5. *All SPOs inside a noncircular ellipse are doubly SPOs. SPTs inside noncircular ellipses are characterized as trajectories connecting, in elliptic coordinates, two different vertexes of their rectangle C_λ . There are 12 classes of SPTs, listed in Table 5.*

Proof. Let O be a r -SPO through a point $(q, p) \in \text{Fix}(r)$ with winding numbers $2 \leq m_1 < m_0$, being m_0 its period. We must prove that there exists another reversor $\check{r} \neq r$ and some index $j \in \mathbb{Z}$ such that $(q_j, p_j) \in \text{Fix}(\check{r})$.

First, let us consider the caustic type E. Then, according to Table 3, we have only four possibilities:

$$r \in \{R_x, f \circ R_x, R_y, f \circ R_y\}. \quad (8)$$

The easiest situation is when $m_0 = 2k + 1$, because we know from the last item in Theorem 1 that

$$(q, p) \in \text{Fix}(R_x) \Leftrightarrow (q_{k+1}, p_{k+1}) = f^{k+1}(q, p) \in \text{Fix}(f \circ R_x),$$

and the same with the couple of associated reversors R_y and $f \circ R_y$. This proves the first row of Table 5. The formulae in the last column are deduced from the symmetry sets in Subsec. 5.3.

Next, we assume that $m_0 = 4k$. That is, we deal with the second row of Table 5. We study each one of the four feasible reversors listed in (8).

- If $r = R_x$, then $q_0 \in \{y\text{-axis}\}$, so $x_0 = 0$. Thus, since $m_0 = 4k$, we have $y_{3k} = y_{-k} = y_k = -y_{3k}$. The last equality follows from Lemma 2a) for $l = 2k$ and $j = k$. The above equalities imply $y_{3k} = y_k = 0$ and thus we can take $\check{r} = R_y$ and $j \in \{k, 3k\}$.
- The case $r = R_y$ is similar. Suffice it to exchange variables x and y .
- The cases $r \in \{f \circ R_x, f \circ R_y\}$ follow directly from the two previous ones by using Corollary 1.

Finally, we assume that $m_0 = 4k + 2$, which corresponds to the third row of Table 5. As before, the four feasible reversors listed in (8) are studied separately.

- If $r = R_x$, then $q_0 \in \{y\text{-axis}\}$, so $x_0 = 0$. Thus, since $m_0 = 4k + 2$, we have $u_{3k+2} = u_{-k} = u_{k+1} = -u_{3k+2}$. The last equality follows from Lemma 2a) for $l = 2k + 1$ and $j = k + 1$. These equalities imply $u_{3k+2} = u_{k+1} = 0$ and thus we can take $\check{r} = f \circ R_y$ and $j \in \{k + 1, 3k + 2\}$.
- The case $r = f \circ R_y$ follows directly from the case $r = R_x$ by using Corollary 1.
- The cases $r \in \{R_y, f \circ R_x\}$ are similar to the previous ones. Suffice it to exchange variables x and y .

The proofs for the three rows about H-caustics follow the same lines, but using Lemma 2b). We skip the details.

Once we know that all SPOs are doubly SPOs, we deduce that, any doubly SPT connects two different vertexes, namely, the ones corresponding to the couple of reversors of the doubly SPT. Indeed, we simply take into account the 1-to-1 correspondence between reversors and vertexes of rectangles \mathcal{C}_λ , as listed in Table 2. Besides, there are $12 = 2 \times 6$ classes of SPTs, since there are two types of caustic (E and H) and any rectangle has four vertexes, and so, six couples of vertexes.

Finally, we check that the 12 classes are *realizable*. That is, we find one SPT of each class. This can be achieved by properly choosing the winding numbers. See Table 5. \square

5.7 Minimal SPTs

We end the study of SPTs inside ellipses by showing an SPT of each one of the 12 classes with the smallest period m_0 . We call *minimal* such SPTs. Therefore, $m_0 \in \{3, 4, 6\}$ for E-caustics, and $m_0 \in \{4, 6\}$ for H-caustics. Period $m_0 = 2$ is discarded, since two-periodic billiard trajectories are singular. The 12 minimal SPTs are drawn in Table 5, both in Cartesian and elliptic coordinates. All of them connect *two* different vertexes of the rectangle \mathcal{C}_λ , as claimed in Theorem 5.

We realize that any minimal SPT of type E has a “twin” of type H when both are depicted in elliptic coordinates.

Type	Period	Minimal SPTs in Cartesian coordinates	Minimal SPTs in elliptic coordinates	Couples of reversors and symmetry properties
E	$2k+1$			$R_x, f \circ R_x$ $q_0 = q_{2k+1} \in \{y\text{-axis}\}$ $p_{k+1} \parallel \{x\text{-axis}\}$ $R_y, f \circ R_y$ $q_0 = q_{2k+1} \in \{x\text{-axis}\}$ $p_{k+1} \parallel \{y\text{-axis}\}$
	$4k$			R_x, R_y $q_0 = q_{4k} = -q_{2k} \in \{y\text{-axis}\}$ $q_{3k} = -q_k \in \{x\text{-axis}\}$ $f \circ R_x, f \circ R_y$ $p_0 = p_{4k} = -p_{2k} \parallel \{x\text{-axis}\}$ $p_{3k} = -p_k \parallel \{y\text{-axis}\}$
	$4k+2$			$R_y, f \circ R_x$ $q_0 = q_{4k+2} = -q_{2k+1} \in \{x\text{-axis}\}$ $p_{3k+2} = -p_{k+1} \parallel \{x\text{-axis}\}$ $R_x, f \circ R_y$ $q_0 = q_{4k+2} = -q_{2k+1} \in \{y\text{-axis}\}$ $p_{3k+2} = -p_{k+1} \parallel \{y\text{-axis}\}$
H	$4k+2$ $\frac{m_1}{2}$ even			$R_x, f \circ R_{xy}$ $q_0 = q_{4k+2} = -q_{2k+1} \in \{y\text{-axis}\}$ $q_{k+1} = -q_k, q_{3k+2} = -q_{3k+1}$ $x_{3k+1} = x_k, y_{3k+1} = -y_k$ $R, f \circ R_y$ $q_0 = (x_0, y_0) = q_{4k+2} \in Q \cap Q_\lambda$ $q_{2k+1} = (x_0, -y_0) \in Q \cap Q_\lambda$ $p_{3k+2} = -p_{k+1} \parallel \{y\text{-axis}\}$
	$4k$			R, R_x $q_0 = q_{4k} = q_{2k} \in \{y\text{-axis}\}$ $q_k = (x_k, y_k) \in Q \cap Q_\lambda$ $q_{3k} = (-x_k, y_k) \in Q \cap Q_\lambda$ $f \circ R_y, f \circ R_{xy}$ $q_0 = q_{4k} = -q_1, q_{2k+1} = -q_{2k}$ $x_{2k} = -x_0, y_{2k} = y_0$ $p_{3k} = -p_k \parallel \{y\text{-axis}\}$
	$4k+2$ $\frac{m_1}{2}$ odd			$R, f \circ R_{xy}$ $q_0 = q_{4k+2} = -q_{2k+1} \in Q \cap Q_\lambda$ $q_{3k+2} = q_k = -q_{k+1} = -q_{3k+1}$ $R_x, f \circ R_y$ $q_0 = q_{4k+2} = -q_{2k+1} \in \{y\text{-axis}\}$ $p_{3k+2} = -p_{k+1} \parallel \{y\text{-axis}\}$

Table 5. Classification and symmetry properties of SPTs together to the minimal SPTs in Cartesian and elliptic coordinates. Black, red, grey, blue and green colors agree in both coordinates. The first three colors also agree with the ones displayed in Fig. 2.

Any SPT, minimal or not, can be computed as follows. First, we fix a caustic type (E or H), a reversor r , a period m_0 (which must be even for H-caustics), and an even winding number m_1 , such that $2 \leq m_1 < m_0$. We have listed in Table 5 all possible combinations. Then we find the caustic parameter through numerical inversion of the relation $\rho(\lambda) = m_1/2m_0$. Of course, we solve that equation for $\lambda \in E$ or $\lambda \in H$, depending on the caustic type we are looking for. Finally, we take from Table 1 the starting point $(q, p) \in \text{Fix}(r)$ such that $q + \langle p \rangle$ is tangent to Q_λ , and iterating the billiard map $f: M \rightarrow M$, we get the whole SPO in the phase space M and the whole SPT in \mathbb{R}^2 .

Any R -SPT is travelled twice in opposite directions, since it hits orthogonally the ellipse at points $q \in Q \cap Q_\lambda$. It can be observed in the last three rows of Table 5. Therefore, there exist SPTs of even period $m_0 = 2l \geq 4$, with only $l + 1$ distinct impact points on the ellipse. We have found similar SPTs inside ellipsoids of \mathbb{R}^3 . See Fig. 1.

Finally, we stress that any SPT has a dual version of the same period and caustic type, given by the dual symmetry g ; see Corollary 1. For instance, this duality is evident for the two SPTs with caustic type E that have common period $m_0 = 4k$. Suffice it to compare the two groups of associated formulae in the second row of Table 5, and to recall that g exchanges the role of positions and velocities. In particular, the rectangular trajectory of that row is the dual version of the diamond-shaped one. The same applies to rows 1, 4 and 5. Instead, trajectories in rows 3 and 6 are dual of themselves.

6 3D case

The previous section sets the basis of this one. Roughly speaking, we apply similar ideas to find analogous results.

6.1 Caustics and elliptic coordinates

Let us recall some classical facts about caustics and elliptic coordinates. All the notations introduced in this subsection will be used later on in this section.

We write the ellipsoid as

$$Q = \left\{ (x_1, x_2, x_3) \in \mathbb{R}^3: \frac{x_1^2}{a_1} + \frac{x_2^2}{a_2} + \frac{x_3^2}{a_3} = 1 \right\}, \quad (9)$$

where $0 < a_1 < a_2 < a_3$. Any nonsingular billiard trajectory inside Q is tangent to two distinct confocal caustics Q_{λ_1} and Q_{λ_2} (with $\lambda_1 < \lambda_2$) of the family

$$Q_\mu = \left\{ (x_1, x_2, x_3) \in \mathbb{R}^3: \frac{x_1^2}{a_1 - \mu} + \frac{x_2^2}{a_2 - \mu} + \frac{x_3^2}{a_3 - \mu} = 1 \right\},$$

where $\mu \notin \{a_1, a_2, a_3\}$. If we set

$$E = (0, a_1), \quad H_1 = (a_1, a_2), \quad H_2 = (a_2, a_3),$$

then Q_μ is an ellipsoid for $\mu \in E$, a one-sheet hyperboloid if $\mu \in H_1$, and a two-sheet hyperboloid when $\mu \in H_2$.

Not all combinations of caustics exist. For instance, both caustics cannot be ellipsoids. The four possible combinations are denoted by EH1, H1H1, EH2, and H1H2. Hence, the caustic parameter $\lambda = (\lambda_1, \lambda_2)$ belongs to the nonsingular caustic space

$$\Lambda = (E \times H_1) \cup (H_1 \otimes H_1) \cup (E \times H_2) \cup (H_1 \times H_2),$$

for $H_1 \otimes H_1 = \{(\lambda_1, \lambda_2) \in H_1 \times H_1: \lambda_1 < \lambda_2\}$, in order to avoid the singular case $\lambda_1 = \lambda_2$.

Let us write the three coordinates planes of \mathbb{R}^3 as

$$\Pi_l = \{(x_1, x_2, x_3) \in \mathbb{R}^3: x_l = 0\}, \quad l \in \{1, 2, 3\}.$$

We know (see Theorem 2) that given any $q \notin \Pi_1 \cup \Pi_2 \cup \Pi_3$, there exist an ellipsoid Q_e , a one-sheet hyperboloid Q_{h_1} and a two-sheet hyperboloid Q_{h_2} such that

$$q \in Q_e \cap Q_{h_1} \cap Q_{h_2}, \quad (10)$$

those being quadrics mutually orthogonal at q . Therefore, $e < a_1 < h_1 < a_2 < h_2 < a_3$. Let $\mathfrak{q} = (e, h_1, h_2)$ be the *elliptic coordinates* of $q = (x_1, x_2, x_3)$. The relation between Cartesian and elliptic coordinates (5) becomes

$$x_i^2 = \frac{(a_i - e)(a_i - h_1)(a_i - h_2)}{(a_i - a_j)(a_i - a_k)}, \quad (11)$$

for any $\{i, j, k\} = \{1, 2, 3\}$. To understand what happens at nongeneric points, we define the three singular caustics as

$$Q_{a_l} = \Pi_l, \quad l \in \{1, 2, 3\}.$$

We also recall that the *focal ellipse* and *focal hyperbola* shared by the family of confocal quadrics $\{Q_\mu: \mu \in \mathbb{R}\}$ are

$$\begin{aligned} \mathcal{E} &= \left\{ (0, x_2, x_3) \in \mathbb{R}^3: \frac{x_2^2}{a_2 - a_1} + \frac{x_3^2}{a_3 - a_1} = 1 \right\} \subset \Pi_1, \\ \mathcal{H} &= \left\{ (x_1, 0, x_3) \in \mathbb{R}^3: \frac{x_3^2}{a_3 - a_2} - \frac{x_1^2}{a_2 - a_1} = 1 \right\} \subset \Pi_2. \end{aligned}$$

These notations are useful because of the following lemma, which is a known extension of the first item in Theorem 2.

Lemma 3. *If $q \notin \mathcal{E} \cup \mathcal{H}$, then there exists $\mathfrak{q} = (e, h_1, h_2)$ such that $e \leq a_1 \leq h_1 \leq a_2 \leq h_2 \leq a_3$, $e \neq h_1$, $h_1 \neq h_2$, and property (10) holds, including its orthogonal character.*

Thus, we can express in elliptic coordinates all points along nonsingular billiard trajectories. The trajectory is contained inside Q , so $e \geq 0$. Impact points $q \in Q$ correspond to $e = 0$. Tangency points $q \in Q_{\lambda_j}$ correspond to $e = \lambda_j \in E$, $h_1 = \lambda_j \in H_1$ or $h_2 = \lambda_j \in H_2$ depending on the type of the caustic Q_{λ_j} . Crossing points $q \in \Pi_l$ have the following elliptic coordinates: Π_1 is $\{e = a_1\} \cup \{h_1 = a_1\}$, Π_2 is $\{h_1 = a_2\} \cup \{h_2 = a_2\}$, and Π_3 is $\{h_2 = a_3\}$.

Indeed, one could agree that $\mathcal{E} = \{e = a_1 = h_1\}$ and $\mathcal{H} = \{h_1 = a_2 = h_2\}$, although we do not need it, because all nonsingular billiard trajectories sharing the caustics Q_{λ_1} and Q_{λ_2} are contained, in elliptic coordinates, inside the cuboid

$$C_\lambda = \begin{cases} [0, \lambda_1] \times [a_1, \lambda_2] \times [a_2, a_3], & \text{for type EH1,} \\ [0, a_1] \times [\lambda_1, \lambda_2] \times [a_2, a_3], & \text{for type H1H1,} \\ [0, \lambda_1] \times [a_1, a_2] \times [\lambda_2, a_3], & \text{for type EH2,} \\ [0, a_1] \times [\lambda_1, a_2] \times [\lambda_2, a_3], & \text{for type H1H2.} \end{cases} \quad (12)$$

We note that $e \neq h_1 \neq h_2$ for all $q = (e, h_1, h_2) \in \mathcal{C}_\lambda$, since $\lambda = (\lambda_1, \lambda_2) \in \Lambda$. Hence, all points belonging to \mathcal{C}_λ verify (10) and (11).

6.2 Frequency map and winding numbers

The following results related to periodic trajectories of billiards inside ellipsoids can be found in [5].

There exists a map $\omega: \Lambda \rightarrow \mathbb{R}^2$, called *frequency map* and defined by means of six hyperelliptic integrals, that characterizes all caustic parameters $\lambda = (\lambda_1, \lambda_2)$ that give rise to periodic trajectories. (Its explicit formula is given in [5].) To be precise, the billiard trajectories sharing the caustics Q_{λ_1} and Q_{λ_2} are periodic if and only if

$$\omega(\lambda_1, \lambda_2) = (m_1, m_2)/2m_0 \in \mathbb{Q}^2 \quad (13)$$

for some positive integers m_0, m_1 , and m_2 . These are the *winding numbers* introduced in item d) of Theorem 4. They describe how trajectories fold in \mathbb{R}^3 . First, m_0 is the period. Second, m_1 is the number of Π_1 -crossings and m_2 is twice the number of turns around the x_1 -axis for EH1-caustics; m_1 is twice the number of turns around the x_3 -axis and m_2 is the number of Π_3 -crossings for EH2-caustics; m_1 is the number of tangential touches with each one-sheet hyperboloid caustic and m_2 is twice the number of turns around the x_1 -axis for H1H1-caustics; whereas m_1 is the number of Π_2 -crossings and m_2 is the number of Π_3 -crossings for H1H2-caustics. Only EH1-caustics and EH2-caustics have trajectories of odd period.

6.3 Reversors and their symmetry sets

Let $\sigma_l, \sigma_{mn}, \sigma_{123}: \mathbb{R}^3 \rightarrow \mathbb{R}^3$ be the $x_m x_n$ -specular reflection, the x_l -axial reflection, and the central reflection, respectively. Here, $\{l, m, n\} = \{1, 2, 3\}$. Two samples are $\sigma_3(x_1, x_2, x_3) = (x_1, x_2, -x_3)$ and $\sigma_{13}(x_1, x_2, x_3) = (-x_1, x_2, -x_3)$. Let $s_l, s_{mn}, s_{123}: M \rightarrow M$ be the symmetries given by $s_l(q, p) = (\sigma_l q, \sigma_l p)$, $s_{mn}(q, p) = (\sigma_{mn} q, \sigma_{mn} p)$, and $s_{123}(q, p) = (\sigma_{123} q, \sigma_{123} p)$. We denote by R the reversor written as \tilde{r} in Sec. 3. Likewise, $R_l = s_l \circ R$, $R_{mn} = \sigma_{mn} \circ R$, and $R_{123} = s_{123} \circ R$.

Remark 4. Henceforth, we shall adopt the following index notation for the sake of brevity. If l, m , and n appear without an explicit explanation of their ranges, it must be understood that they represent *any* choice such that $\{l, m, n\} = \{1, 2, 3\}$. This convention is used, for instance, in Tables 6 and 7. Moreover, in the second to fifth rows of Table 7, index l has a distinguished meaning from indexes m and n ; and the formulae contained in those rows are invariant under permutation of m and n . This has to do with the fact that $\sigma_{mn} = \sigma_{nm}$.

The three planar sections of the ellipsoid are

$$S_l = Q \cap \Pi_l, \quad l \in \{1, 2, 3\}.$$

The symmetry sets of the $16 = 2^4$ reversors are listed in Table 6, which follows directly from Proposition 2. We note that only the symmetry sets of R_{123} and $f \circ R$ are empty. We usually write coordinates $q = (x_1, x_2, x_3)$ in the configuration space Q , and $p = (u_1, u_2, u_3)$ in the velocity space \mathbb{S}^2 .

r	$\text{Fix}(r)$	$\text{Fix}(f \circ r)$
R	$p \in N_q Q$	\emptyset
R_l	$q \in S_l$ and $p \in N_q S_l$	$u_m = u_n = 0, u_l^2 = 1$
R_{mn}	$x_m = x_n = 0, x_l^2 = a_l$	$(q + \langle p \rangle) \perp_* \{x_l\text{-axis}\}$
R_{123}	\emptyset	$0 \in q + \langle p \rangle$

Table 6. The symmetry sets of the 16 reversors of the billiard inside a triaxial ellipsoid $Q \subset \mathbb{R}^3$.

6.4 Characterization of STs

We want to characterize nonsingular STs inside nondegenerate ellipsoids, as trajectories passing, in elliptic coordinates, through some vertex of the cuboid \mathcal{C}_λ . In order to accomplish this goal, we must prove both implications. In Proposition 5 we check that any vertex of \mathcal{C}_λ is visited by some (indeed, eight) STs. In Proposition 6 we see that any ST passes through some vertex of \mathcal{C}_λ .

Proposition 5. *Let $\lambda = (\lambda_1, \lambda_2) \in \Lambda$ be fixed. Given any vertex $q_* = (e, h_1, h_2)$ of \mathcal{C}_λ , let $q_* \in Q_e \cap Q_{h_1} \cap Q_{h_2}$. Then there exists some reversor r , and some point $(q, p) \in \text{Fix}(r)$ such that $q_* \in q + \langle p \rangle$ and the line $q + \langle p \rangle$ is tangent to Q_{λ_1} and Q_{λ_2} . If $e = 0$, $q = q_*$; otherwise q_* is the middle point of the consecutive impact points \hat{q} and q .*

We clarify some aspects of this result before its proof:

- We follow the index notation explained in remark 4.
- We know that two symmetry sets only intersect at points $(q, p) \in M$ such that the line $q + \langle p \rangle$ is contained in some coordinate plane; see Proposition 2. But we are dealing with nonsingular trajectories. Therefore, we can associate just one reversor to each vertex.
- The correspondence $q_* \mapsto (q, p)$ is 1-to-8 (cf. Table 7). This has to do with two facts. First, elliptic coordinates do not distinguish among the eight octants in \mathbb{R}^3 . Moreover, unit velocities p directed inward Q at impact points q are excluded from Table 7; otherwise, $(q, p) \notin M$. The billiard trajectory associated to any of those eight points (q, p) of the phase space is r -symmetric and passes, in elliptic coordinates, through vertex q_* .

Proof. To begin with, we know from Lemma 3 that Q_e, Q_{h_1} and Q_{h_2} are mutually orthogonal at q_* . There are several kinds of vertexes. The first distinction is $e = 0$ or $e \neq 0$; that is, $q_* \in Q$ or $q_* \notin Q$. The second distinction is the number of coordinate planes through q_* . It turns out that there are six kinds of vertexes. We study each kind separately.

- If the point q_* belongs to Q but is outside all three coordinate planes, then $q_* = (0, \lambda_1, \lambda_2)$. From (12), the type is H1H2. Thus, Q_{λ_1} is a one-sheet hyperboloid, Q_{λ_2} is a two-sheet hyperboloid, and Q, Q_{λ_1} and Q_{λ_2} are pairwise orthogonal at $q = q_*$. Thus, if p is the outward unit normal velocity to Q at q , then $(q, p) \in \text{Fix}(R)$ and the line $q + \langle p \rangle$ is tangent to Q_{λ_1} and Q_{λ_2} . Finally, let us check the formulae for q and p given in Table 7.

Vertex $q_\star = (e, h_1, h_2)$	Type	q_\star belongs to	r	$q = (x_1, x_2, x_3), p = (u_1, u_2, u_3)$
$(0, \lambda_1, \lambda_2)$	H1H2	$Q \cap Q_{\lambda_1} \cap Q_{\lambda_2}$	R	$x_l^2 = \frac{a_l(a_l - \lambda_1)(a_l - \lambda_2)}{(a_l - a_m)(a_l - a_n)}, u_l = \frac{x_l}{a_l} \sqrt{\frac{a_1 a_2 a_3}{\lambda_1 \lambda_2}}$
$e = 0, \{h_1, h_2\} = \{a_i, \lambda_j\}$	all	$Q \cap \Pi_l \cap Q_{\lambda_j}$	R_l	$x_l = 0, x_m^2 = \frac{a_m(a_m - \lambda_j)}{a_m - a_n}, x_n^2 = \frac{a_n(a_n - \lambda_j)}{a_n - a_m}$ $u_l^2 = \frac{a_l - \lambda_k}{a_l}, (u_m, u_n) = \sqrt{\frac{\lambda_k}{a_1 a_2 a_3 \lambda_j}} (a_n x_m, a_n x_m)$
$e = 0, \{h_1, h_2\} = \{a_m, a_n\}$	not H1H1	$Q \cap \Pi_m \cap \Pi_n$	R_{mn}	$x_l^2 = a_l, x_m = x_n = 0, u_l^2 = \frac{\lambda_1 \lambda_2}{a_m a_n}, \text{sign}(u_l) = \text{sign}(x_l)$ $u_m^2 = \frac{(a_m - \lambda_1)(a_m - \lambda_2)}{a_m(a_m - a_n)}, u_n^2 = \frac{(a_n - \lambda_1)(a_n - \lambda_2)}{a_n(a_n - a_m)}$
$\{e, h_1, h_2\} = \{a_l, \lambda_1, \lambda_2\}$	not H1H1	$\Pi_l \cap Q_{\lambda_1} \cap Q_{\lambda_2}$	$f \circ R_l$	$u_l^2 = 1, u_m = u_n = 0, x_l^2 = \frac{a_l \lambda_1 \lambda_2}{a_m a_n}, \text{sign}(u_l) = \text{sign}(x_l)$ $x_m^2 = \frac{(a_m - \lambda_1)(a_m - \lambda_2)}{a_m - a_n}, x_n^2 = \frac{(a_n - \lambda_1)(a_n - \lambda_2)}{a_n - a_m}$
$\{e, h_1, h_2\} = \{a_m, a_n, \lambda_j\}$	all	$\Pi_m \cap \Pi_n \cap Q_{\lambda_j}$	$f \circ R_{mn}$	$u_l = 0, u_m^2 = \frac{a_m - \lambda_j}{a_m - a_n}, u_n^2 = \frac{a_n - \lambda_j}{a_n - a_m}$ $x_l^2 = a_l - \lambda_k, (x_m, x_n) = \sqrt{\frac{a_m a_n \lambda_k}{a_l \lambda_j}} (u_m, u_n)$
(a_3, a_2, a_1)	H1H2	$\Pi_3 \cap \Pi_2 \cap \Pi_1$	$f \circ R_{123}$	$u_l^2 = \frac{(a_l - \lambda_1)(a_l - \lambda_2)}{(a_l - a_m)(a_l - a_n)}, x_l = \sqrt{\frac{a_1 a_2 a_3}{\lambda_1 \lambda_2}} u_l$

Table 7. Relations among vertexes q_\star of the cuboid \mathcal{C}_λ , types of caustics, reversors r , and points $q_\star \in q + \langle p \rangle$ such that $q + \langle p \rangle$ is tangent to Q_{λ_1} and Q_{λ_2} , with $(q, p) \in \text{Fix}(r)$. Notation for indexes $\{l, m, n\} = \{1, 2, 3\}$ and $\{j, k\} = \{1, 2\}$ is described in the text.

The formula for q follows directly from (11). Thus, there are exactly eight choices for q . If $p \in N_q Q$ and p points outward Q at q , then there exists $\mu > 0$ such that $u_l = \mu x_l / a_l$. And using that $p \in \mathbb{S}^2$ we get that

$$1 = \mu^2 \left(\frac{x_1^2}{a_1^2} + \frac{x_2^2}{a_2^2} + \frac{x_3^2}{a_3^2} \right) \Rightarrow \mu = \sqrt{\frac{a_1 a_2 a_3}{\lambda_1 \lambda_2}}.$$

In summary, only R -STs with H1H2-caustics can take place for this vertex.

- b) If the point q_\star belongs to Q and is contained in only one coordinate plane, say Π_l , then $q_\star = (0, h_1, h_2)$ with $\{h_1, h_2\} = \{a_i, \lambda_j\}$ for some $j \in \{1, 2\}$. In that case, $q_\star \in Q \cap \Pi_l \cap Q_{\lambda_j} = S_l \cap Q_{\lambda_j}$. We do not get any restriction on the type of the caustics, but only some restrictions on the indexes; see (12). Namely,

- $l \in \{2, 3\}$ and $j = 2$ for type EH1;
- $l \in \{2, 3\}$ for type H1H1;
- $l \in \{1, 2\}$ and $j = 2$ for type EH2; and
- $l = j = 2$ or $(l, j) = (3, 1)$ for type H1H2.

We observe that any $(q, p) \in M$ such that $q = q_\star$ and $p \in N_q S_l$ is contained in $\text{Fix}(R_l)$. Thus, the formula for q follows again from relations (11), and we find four choices for q . Next, we look for an outward velocity $p = (u_1, u_2, u_3) \in \mathbb{S}^2$ such that $p \perp T_q S_l$ and $q + \langle p \rangle$ is tangent to both Q_{λ_j} and Q_{λ_k} with $\{j, k\} = \{1, 2\}$.

Condition $p \perp T_q S_l$ reads as $x_n u_m / a_n = x_m u_n / a_m$. In other words, we look for some $\nu \in \mathbb{R}$ such that

$$(u_m, u_n) = \nu (a_n x_m, a_m x_n).$$

Then, tangency with Q_{λ_j} is immediate, since Q_{λ_j} is orthogonal to the planar section $S_l = Q \cap \Pi_l$ at q . It only remains to impose the tangency with Q_{λ_k} . Thus, the quadratic equation

$$\frac{(x_l + t u_l)^2}{a_l - \lambda_k} + \frac{(x_m + t u_m)^2}{a_m - \lambda_k} + \frac{(x_n + t u_n)^2}{a_n - \lambda_k} = 1$$

must have a unique solution in t , which is equivalent to the vanishing of its discriminant: $\beta^2 = \alpha \gamma$, where

$$\begin{aligned} \alpha &= \frac{u_l^2}{a_l - \lambda_k} + \frac{u_m^2}{a_m - \lambda_k} + \frac{u_n^2}{a_n - \lambda_k} \\ &= \frac{1}{a_l - \lambda_k} \left(1 + \left(\frac{a_l - a_m}{a_m - \lambda_k} a_n^2 x_m^2 + \frac{a_l - a_n}{a_n - \lambda_k} a_m^2 x_n^2 \right) \nu^2 \right), \\ \beta &= \frac{x_m u_m}{a_m - \lambda_k} + \frac{x_n u_n}{a_n - \lambda_k} = \frac{a_m a_n (\lambda - \beta) \nu}{(a_m - \lambda_k)(a_n - \lambda_k)}, \\ \gamma &= \frac{x_m^2}{a_m - \lambda_k} + \frac{x_n^2}{a_n - \lambda_k} - 1 = \frac{\lambda_k (\lambda_j - \lambda_k)}{(a_m - \lambda_k)(a_n - \lambda_k)}. \end{aligned}$$

Here, we have used that $u_l^2 = 1 - u_m^2 - u_n^2$. After some calculations we find $\nu^2 = \lambda_k / \lambda_j a b c$, and from here we get the desired formulae in Table 7. We must impose in turn, that p is an outward velocity, so

$$0 < \langle Dq, p \rangle = \nu (a_n x_m^2 / a_m + a_m x_n^2 / a_n),$$

and $\nu > 0$. Thus, once we fix q , there are two choices for u_l , and exactly eight choices for (q, p) .

We finish this item by stressing the consequences of the restrictions on the index l . They mean that the reversor R_1 cannot take place for types EH1, H1H1, and H1H2, whereas R_3 is forbidden for type EH2. This information is displayed in Table 9.

- c) If q_\star belongs to Q and is contained in two coordinate planes, say Π_m and Π_n , then $q_\star = (0, h_1, h_2)$ with $\{h_1, h_2\} = \{a_m, a_n\}$. This prevents H1H1-caustics, see (12). Furthermore, we get again some restrictions on the indexes, see (12). Namely,

- $1 \in \{m, n\}$ for type EH1;
- $3 \in \{m, n\}$ for type EH2; and
- $1 \notin \{m, n\}$ for type H1H2.

Besides, q_* is one of the two vertexes of the ellipsoid on the x_l -axis. Therefore, any $(q, p) \in M$ such that $q = q_*$ is contained in $\text{Fix}(R_{mn})$. Finally, let us check that the formulae given for $p = (u_1, u_2, u_3)$ in Table 7 are correct.

We look for an outward velocity $p \in \mathbb{S}^2$ such that the line $q + \langle p \rangle$ is tangent to Q_{λ_k} , for $k = 1, 2$. Thus, the quadratic equation

$$\frac{(x_l + tu_l)^2}{a_l - \lambda_k} + \frac{(x_m + tu_m)^2}{a_m - \lambda_k} + \frac{(x_n + tu_n)^2}{a_n - \lambda_k} = 1$$

must have a unique solution in t , which is equivalent to the vanishing of its discriminant: $\beta^2 = \alpha\gamma$, where

$$\begin{aligned} \alpha &= \frac{u_l^2}{a_l - \lambda_k} + \frac{u_m^2}{a_m - \lambda_k} + \frac{u_n^2}{a_n - \lambda_k} \\ &= \frac{1}{a_n - \lambda_k} \left(1 + \frac{a_n - a_l}{a_l - \lambda_k} u_l^2 + \frac{a_n - a_m}{a_m - \lambda_k} u_m^2 \right), \\ \beta &= \frac{x_l u_l}{a_l - \lambda_k}, \\ \gamma &= \frac{x_l^2}{a_l - \lambda_k} - 1 = \frac{\lambda_k}{a_l - \lambda_k}. \end{aligned}$$

After some calculations we obtain that

$$a_n(a_m - \lambda_k)u_l^2 + (a_m - a_n)\lambda_k u_m^2 = \lambda_k(a_m - \lambda_k).$$

for $k = 1, 2$. These two equations along with condition $u_l^2 + u_m^2 + u_n^2 = 1$ form a system of three linear equations in the unknowns u_l^2 , u_m^2 , and u_n^2 . A simple computation shows that the formulae given in Table 7 are the unique solution of this system.

Finally, we impose that p is an outward velocity, so

$$0 < \langle Dq, p \rangle = x_l u_l / a_l,$$

and $x_l u_l > 0$. Thus, once fixed the vertex q , there are two choices for u_m and two others for u_n . Therefore, there are exactly eight choices for (q, p) .

We finish again by stressing the consequences of the restrictions on the indexes m and n . They mean that the reversor R_{23} cannot take place for type EH1, R_{12} is forbidden for type EH2, both R_{13} and R_{12} are not allowed for type H1H2, and all reversors of the form R_{mn} cannot be found for type H1H1. This information is also displayed in Table 9.

- d) If q_* does not belong to Q but it is in all coordinate planes, then $q_* = (0, 0, 0) = 0$ and $q_* = (a_3, a_2, a_1)$. In that case the type is H1H2; see (12). We look for lines $q_* + \langle p \rangle = \langle p \rangle$ that are tangent to the one-sheet hyperboloid Q_{λ_1} and to the two-sheet hyperboloid Q_{λ_2} . Since q_* is the center of both quadrics, $p = (u_1, u_2, u_3)$ must be an asymptotic direction of them, so

$$\frac{u_1^2}{a_1 - \lambda_k} + \frac{u_2^2}{a_2 - \lambda_k} + \frac{u_3^2}{a_3 - \lambda_k} = 0, \quad k \in \{1, 2\}.$$

These equations along with $u_l^2 + u_m^2 + u_n^2 = 1$ form a system of three linear equations in the unknowns u_l^2 , u_m^2 , and u_n^2 . A simple computation shows that the formulae given in Table 7 are the unique solution of this system. Thus, there are exactly eight choices for p .

The line $q_* + \langle p \rangle = 0 + \langle p \rangle$ intersects the ellipsoid Q at some points $q = \mu p$ and $\hat{q} = -\mu p$ where $\mu > 0$. So, $x_l = \mu u_l$. And using that $q \in Q$ we get that

$$1 = \mu^2 \left(\frac{u_1^2}{a_1^2} + \frac{u_2^2}{a_2^2} + \frac{u_3^2}{a_3^2} \right) \Rightarrow \mu = \sqrt{\frac{a_1 a_2 a_3}{\lambda_1 \lambda_2}}.$$

Finally, we realize that $(q, p) \in \text{Fix}(R_{123})$ and q_* is the middle point of \hat{q} and q .

In summary, only $f \circ R_{123}$ -STs with H1H2-caustics can take place for this vertex.

- e) If q_* does not belong to Q but it is two coordinate planes, say Π_m and Π_n , then $q_* = (e, h_1, h_2)$ with $\{e, h_1, h_2\} = \{a_m, a_n, \lambda_j\}$. This case is the “dual” of case b), so it is associated to the reversors $f \circ R_{mn}$. The computations do not involve new ideas. We skip them. We just stress that there are no restriction on the type of the caustics, but only some restrictions on the indexes, see (12). Namely,

- $1 \in \{m, n\}$ for types EH1, H1H1, and H1H2; and
- $3 \in \{m, n\}$ for types EH2.

They mean that the reversor $f \circ R_{23}$ cannot take place for types EH1, H1H1, and H1H2, whereas $f \circ R_{12}$ is forbidden for type EH2.

- f) If q_* does not belongs to Q and is contained in only one coordinate plane, say Π_l , then $q_* = (e, h_1, h_2)$ with $\{h_1, h_2\} = \{a_l, \lambda_1, \lambda_2\}$. In that case, $q_* \in \Pi_l \cap Q_{\lambda_1} \cap Q_{\lambda_2}$. This case is the “dual” of case c), so it is associated to the reversors $f \circ R_l$. We also skip the computations.

We only remark that no H1H1-caustics can be associated to this case. Besides, we get again some restrictions on the indexes, see (12). Namely, $l \neq 1$ for type EH1; $l \neq 3$ for type EH2; and $l = 1$ for type H1H2. Consequently, $f \circ R_1$ cannot take place for type EH1, $f \circ R_3$ is forbidden for type EH2, both $f \circ R_2$ and $f \circ R_3$ are not allowed for type H1H2, and all reversors of the form $f \circ R_l$ cannot be found for type H1H1. \square

Remark 5. Opposed vertexes of a given cuboid \mathcal{C}_λ provide points on dual symmetry sets. At the same time, the formulae for (q, p) of reversors $f \circ R_l$, $f \circ R_{mn}$ and $f \circ R_{123}$ follow from the formulae of their dual reversors R_{mn} , R_l and R , respectively, by the change $u_i^2 \leftrightarrow x_i^2/a_i$. This does not come as a surprise; see Corollary 1. Suffice it to realize that the dual symmetry $g: M \rightarrow M$, $g(q, p) = (\bar{q}, \bar{p})$, verifies that $\bar{p} = -C^{-1}q$, with $C^2 = \text{diag}(a_1, a_2, a_3)$.

All implications in the proof of Proposition 5 can be reversed. Hence, we can move along Table 7 in both directions: from left to right and from right to left.

Nevertheless, we prefer to prove Proposition 6 following a reasoning whose generalization to an arbitrary dimension is straightforward.

Proposition 6. *Let O be a nonsingular r -SO through a point $(q, p) \in \text{Fix}(r)$ for some reversor $r: M \rightarrow M$. Let $\lambda = (\lambda_1, \lambda_2) \in \Lambda$ be its caustic parameter. Then there exists a vertex $q_* = (e, h_1, h_2)$ of the cuboid \mathcal{C}_λ and a point $q_* \in Q_e \cap Q_{h_1} \cap Q_{h_2}$ such that $q_* \in q + \langle p \rangle$.*

Proof. First, we consider the reversors of the form R , R_l or R_{mn} . Let $\tilde{q}: \mathbb{R} \rightarrow \mathbb{R}^3$, $\tilde{q}(t) = (\tilde{x}_1(t), \tilde{x}_2(t), \tilde{x}_3(t))$, be the arc-length parameterization of the billiard trajectory through the impact point $q_* = q$ with unit velocity p . Clearly, it is smooth except at impact points. Besides, it has the symmetry properties listed in Table 8, which can be deduced from comments after Remark 2 and elementary geometric arguments.

r	Symmetry property
R	$\tilde{q}(-t) = \tilde{q}(t)$
R_l	$\tilde{q}(-t) = \sigma_l \tilde{q}(t)$
R_{mn}	$\tilde{q}(-t) = \sigma_{mn} \tilde{q}(t)$
$f \circ R_l$	$\tilde{q}(-t) = \sigma_l \tilde{q}(t)$
$f \circ R_{mn}$	$\tilde{q}(-t) = \sigma_{mn} \tilde{q}(t)$
$f \circ R_{123}$	$\tilde{q}(-t) = -\tilde{q}(t)$

Table 8. Symmetry properties of the arc-length parameterizations of r -STs when $\tilde{q}(0) = q_*$.

Let $\tilde{q}: \mathbb{R} \rightarrow \mathcal{C}_\lambda$, $\tilde{q}(t) = (\tilde{e}(t), \tilde{h}_1(t), \tilde{h}_2(t))$, be the corresponding parameterization in elliptic coordinates. We know that components $\tilde{e}(t)$, $\tilde{h}_1(t)$, and $\tilde{h}_2(t)$, oscillate in some intervals in such a way that their only critical points are attained at the extremes of these intervals. The cuboid \mathcal{C}_λ is the product of these three intervals. Besides, the functions $\tilde{h}_1(t)$ and $\tilde{h}_2(t)$ are smooth everywhere.

The above symmetries of $\tilde{q}(t)$ imply that $\tilde{q}(-t) = \tilde{q}(t)$, since elliptic coordinates do not distinguish among the eight octants in \mathbb{R}^3 . Therefore,

$$\tilde{h}'_1(0) = 0, \quad \tilde{h}'_2(0) = 0.$$

In addition, $\tilde{e}(0) = 0$, since we have taken $q_* = q \in Q$. Hence, $q_* = (e, h_1, h_2) := \tilde{q}(0) = (0, \tilde{h}_1(0), \tilde{h}_1(0))$ is a vertex of \mathcal{C}_λ ; see item c) of Theorem 4.

It remains to consider reversors of the form $f \circ R_l$, $f \circ R_{mn}$ and $f \circ R_{123}$. Let $\tilde{q}: \mathbb{R} \rightarrow \mathbb{R}^3$ be the arc-length parameterization of the billiard trajectory that begins at the middle point $q_* := (q + \hat{q})/2$ with unit velocity p . We recall that \hat{q} is the previous impact point, that is, $Q \cap (q + \langle p \rangle) = \{q, \hat{q}\}$.

The symmetry properties of these parameterizations are also listed in Table 8. For instance, if $r = f \circ R_{123}$, then $q_* = (0, 0, 0)$, which implies $\tilde{q}(-t) = -\tilde{q}(t)$. Then, we apply exactly the same argument as before, with just one difference. The function $\tilde{e}(t)$ is smooth at $t = 0$, because $\tilde{q}(0) = q_* \notin Q$ and $\tilde{e}(0) \neq 0$. Hence, we also get that $\tilde{e}'(0) = 0$, so $q_* = (e, h_1, h_2) := \tilde{q}(0) = (\tilde{e}(0), \tilde{h}_1(0), \tilde{h}_1(0))$ is a vertex of \mathcal{C}_λ .

Property $q_* \in Q_e \cap Q_{h_1} \cap Q_{h_2}$ follows from Lemma 3. \square

Corollary 2. *Nonsingular STs inside triaxial ellipsoids of \mathbb{R}^3 are characterized as trajectories passing, in elliptic coordinates, through some vertex of their cuboid.*

6.5 Forbidden reversors for each type of caustics

Next, we emphasize that, although there are 14 nonempty symmetry sets, once fixed the caustic type, some of them cannot take place. To be more precise, there are ten forbidden symmetry sets for H1H1-caustics, but only six otherwise. These results have been obtained along the proof of Proposition 5, and we organize them in Table 9.

Type	Forbidden reversors
EH1	$R, f \circ R_{123}, R_1, f \circ R_{23}, R_{23}, f \circ R_1$
EH2	$R, f \circ R_{123}, R_3, f \circ R_{12}, R_{12}, f \circ R_3$
H1H1	$R, f \circ R_{123}, R_1, f \circ R_{23}, R_{23}, f \circ R_1, R_{13}, f \circ R_2, R_{12}, f \circ R_3$
H1H2	$R_1, f \circ R_{23}, R_{13}, f \circ R_2, R_{12}, f \circ R_3$

Table 9. Forbidden reversors for each type of caustics.

Forbidden reversors appear in *dual couples* —couples whose symmetry sets are interchanged by the symmetry g .

A glance at cuboid (12) and Table 7 shows that, two different vertexes of the same cuboid cannot be associated to the same reversor, but in one case: H1H1-caustics. This agrees with the previous digression, where we found 8 = 14 – 6 feasible symmetry sets for caustics of type EH1, EH2, and H1H2, but only 4 = 14 – 10 for H1H1-caustics.

6.6 Characterization and classification of SPTs

Let us characterize and classify SPTs inside triaxial ellipsoids of \mathbb{R}^3 . We classify them by the caustic type and the couple of vertexes of the cuboid they connect.

Theorem 6. *Nonsingular SPTs inside triaxial ellipsoids of \mathbb{R}^3 are characterized as trajectories connecting, in elliptic coordinates, two different vertexes of their cuboid. All nonsingular SPOs are doubly SPOs, but a few with H1H1-caustics. Besides, there are exactly 112 classes of nonsingular SPTs, listed in Tables 10–13.*

Proof. Let O be a nonsingular r -SPO through a point $(q, p) \in \text{Fix}(r)$, for some reversor $r: M \rightarrow M$, with winding numbers m_0, m_1, m_2 . Let $\lambda = (\lambda_1, \lambda_2) \in \Lambda$ be its caustic parameter. Let L_0 be its length.

Let $\tilde{q}: \mathbb{R} \rightarrow \mathbb{R}^3$ be the arc-length parameterization of the billiard trajectory that begins at the distinguished point q_* introduced in Proposition 6.

Let $\tilde{q}: \mathbb{R} \rightarrow \mathcal{C}_\lambda$ be the corresponding parameterization in elliptic coordinates. Then $\tilde{q}(t)$ is even —see the proof of Proposition 6— and L_0 -periodic —see Theorem 4.

The key trick is as simple as to realize that

$$\tilde{q}(L_0/2 - t) = \tilde{q}(t - L_0/2) = \tilde{q}(t + L_0/2), \quad t \in \mathbb{R}.$$

Hence, $\tilde{q}(t)$ is even with regard to $L_0/2$, and so

$$q_* = (e^*, h_1^*, h_2^*) := \tilde{q}(0), \quad q_\bullet = (e^\bullet, h_1^\bullet, h_2^\bullet) := \tilde{q}(L_0/2)$$

are vertexes of the cuboid \mathcal{C}_λ . The proof for q_* was already explained in Proposition 6, the proof for q_\bullet is equal.

Now, taking into account the interpretation of the winding numbers as, the number of complete oscillations of each elliptic coordinate when the arc-length parameter t moves from 0 to L_0 —see item d) of Theorem 4—, we consider two cases:

- If some winding number is odd, then $q_\bullet \neq q_*$, because

$$e^* = e^\bullet \Leftrightarrow m_0 \in 2\mathbb{Z}, \quad h_i^* = h_i^\bullet \Leftrightarrow m_i \in 2\mathbb{Z}.$$

- If all winding numbers are even, then $\tilde{q}(t)$ has period $L_0/2$ and $q_\bullet = q_*$ —see item d)iii of Theorem 4—, in which case we repeat the same strategy to find a second vertex $q_\circ = (e^\circ, h_1^\circ, h_2^\circ) := \tilde{q}(L_0/4)$ such that

$$e^* = e^\circ \Leftrightarrow m_0 \in 4\mathbb{Z}, \quad h_i^* = h_i^\circ \Leftrightarrow m_i \in 4\mathbb{Z}.$$

Then, $q_\circ \neq q_*$ —see item d)iv of Theorem 4.

Therefore, the trajectory connects two different vertexes in both cases. Next, we prove that any trajectory $\tilde{q}(t)$ connecting, in elliptic coordinates, two vertexes is an SPT. Thus, we assume that $q_* = \tilde{q}(t_*)$ and $q_\bullet = \tilde{q}(t_\bullet)$ are two different vertexes with $t_* < t_\bullet$. From Proposition 5 we know that this trajectory is r_* -symmetric and r_\bullet -symmetric for some reversors r_* and r_\bullet . The case $r_* = r_\bullet$ is not excluded. Repeating the reasoning in Proposition 6, we deduce that $\tilde{q}(t)$ is symmetric with regard to $t = t_*$ and $t = t_\bullet$. In particular, $\tilde{q}(2t_* + t) = \tilde{q}(-t)$ and $\tilde{q}(2t_\bullet + t) = \tilde{q}(-t)$. Set $T = 2(t_\bullet - t_*)$. Then

$$\tilde{q}(t + T) = \tilde{q}(2t_\bullet + t - 2t_*) = \tilde{q}(2t_* - t) = \tilde{q}(t), \quad t \in \mathbb{R}.$$

Hence, $\tilde{q}(t)$ is T -periodic, and so, $\tilde{q}(t)$ is periodic with period T or $2T$; see item d) of Theorem 4. This proves the characterization of SPTs.

Once we have established that any SPT connects two different vertexes of its cuboid, it is easy to deduce that, all SPOs inside triaxial ellipsoids of \mathbb{R}^3 whose type of caustics are EH1, EH2 or H1H2, must be doubly SPOs. Suffice it to recall that each vertex of the cuboid is associated to a different reversor for those three types.

The number 112 comes from 4×28 , since there are 4 types of caustics and any 3-dimensional cuboid has eight vertexes, and so $28 = (8 \times 7)/2$ couples of vertexes.

We must check that none of the 112 classes of SPTs is fictitious. To do it, we present an algorithm that provides a minimal SPT of each class. *Minimal* means that it has the smallest possible period. The key step of the algorithm is to properly choose the winding numbers (m_0, m_1, m_2) . In accordance with the previous discussion, we distinguish four kinds of winding number. Namely, even: “e”, odd: “o”, multiple of four: “f”, and even but not multiple of four: “t”. For instance, all winding numbers of kind (t, t, t) connect opposite vertexes of their cuboids. The kind (f, f, f) never takes place —see item d)iv of Theorem 4.

Let us explain the algorithm by using an example. We want to connect opposite vertexes $\mathbf{q}_* = (e^*, h_1^*, h_2^*) = (0, \lambda_2, a_3)$ and $\mathbf{q}_\bullet = (e^\bullet, h_1^\bullet, h_2^\bullet) = (\lambda_1, a_1, a_2)$ of the cuboid

$$\mathcal{C}_\lambda = [0, \lambda_1] \times [a_1, \lambda_2] \times [a_2, a_3],$$

which corresponds to caustic type EH1.

This problem about vertexes is equivalent to find a periodic trajectory R_3 -symmetric and $f \circ R_{12}$ -symmetric of type EH1, because the reversors associated to \mathbf{q}_* and \mathbf{q}_\bullet are R_3 and $f \circ R_{12}$, respectively (cf. Table 7). As we said above, winding numbers must be of kind (t, t, t). Then, taking for granted conjecture (6), the minimal choice is $(m_0, m_1, m_2) = (10, 6, 2)$. Finally, if we solve equation (13) for $\lambda = (\lambda_1, \lambda_2) \in E \times H_1$, with $(m_0, m_1, m_2) = (10, 6, 2)$, and draw the billiard trajectory through the point (q, p) , given by the formulae of the second row of Table 7 for $l=3$, then we obtain a trajectory of period 10, type EH1, R_3 -symmetric, and $f \circ R_{12}$ -symmetric.

All winding numbers of kind (t, t, t) connect opposite vertexes of their cuboids. Hence, their SPTs of type EH1 can display the following double symmetries: $\{R_3, f \circ R_{12}\}$, $\{R_2, f \circ R_{13}\}$, $\{R_{13}, f \circ R_2\}$, or $\{R_{12}, f \circ R_3\}$. They are obtained by looking in Table 7 the relations between vertexes and reversors.

Other kinds of winding numbers and other caustic types can be studied in a completely analogous way. And so, we complete Tables 10–13. \square

The caustic type H1H1 has the following peculiarity: both caustics Q_{λ_1} and Q_{λ_2} are 1-sheet hyperboloids. We will denote Q_{λ_1} as the outer hyperboloid and Q_{λ_2} as the inner one, since $\lambda_1 < \lambda_2$. Note that two vertexes of the form (e, λ_1, h_2) and (e, λ_2, h_2) are associated to the same reversor; see Table 7. In particular, SPTs connecting vertexes of this form are not doubly symmetric. Likewise, different connections can give rise to the same couple of reversors. We still classify those connections as different classes, because they have different geometries. Symbols $(R_2, R_3 |)$, $(R_3 | R_2)$, $(R_2 | R_3)$, and $(| R_2, R_3)$ denote four classes with caustic type H1H1 and the same couple of reversors: $\{R_2, R_3\}$. They are depicted in Fig. 17. But the

points \mathbf{q}_* , associated to each reversor (Table 7) are on the outer (respectively, inner) hyperboloid when the reversor is written to the left (respectively, right) of symbol $|$. This notation is used in Table 13.

(m_0, m_1, m_2) kind/minimal	Couples of reversors
(t, t, t)	$\{R_3, f \circ R_{12}\}, \{R_2, f \circ R_{13}\}$
(10, 6, 2)	$\{R_{13}, f \circ R_2\}, \{R_{12}, f \circ R_3\}$
(t, t, f)	$\{R_3, f \circ R_{13}\}, \{R_2, f \circ R_{12}\}$
(10, 6, 4)	$\{R_{13}, f \circ R_3\}, \{R_{12}, f \circ R_2\}$
(t, f, t)	$\{R_3, f \circ R_2\}, \{R_2, f \circ R_3\}$
(6, 4, 2)	$\{R_{13}, f \circ R_{12}\}, \{R_{12}, f \circ R_{13}\}$
(o, e, e)	$\{R_3, f \circ R_3\}, \{R_2, f \circ R_2\}$
(5, 4, 2)	$\{R_{13}, f \circ R_{13}\}, \{R_{12}, f \circ R_{12}\}$
(f, t, t)	$\{R_3, R_{12}\}, \{f \circ R_3, f \circ R_{13}\}$
(8, 6, 2)	$\{R_2, R_{13}\}, \{f \circ R_2, f \circ R_{13}\}$
(f, t, f)	$\{R_3, R_{13}\}, \{f \circ R_3, f \circ R_{13}\}$
(8, 6, 4)	$\{R_2, R_{12}\}, \{f \circ R_2, f \circ R_{12}\}$
(f, f, t)	$\{R_3, R_2\}, \{f \circ R_3, f \circ R_2\}$
(8, 4, 2)	$\{R_{13}, R_{12}\}, \{f \circ R_{13}, f \circ R_{12}\}$

Table 10. Classification of SPTs for caustic type EH1. Notation for kinds “e”, “o”, “f”, and “t” is described in the text. For each kind of winding numbers we list its minimal representative, and its four couples of reversors, whose order inside the couple is irrelevant.

(m_0, m_1, m_2) kind/minimal	Couples of reversors
(t, t, t)	$\{R_1, f \circ R_{23}\}, \{R_2, f \circ R_{13}\}$
(10, 6, 2)	$\{R_{13}, f \circ R_2\}, \{R_{23}, f \circ R_1\}$
(t, t, f)	$\{R_1, f \circ R_2\}, \{R_2, f \circ R_1\}$
(10, 6, 4)	$\{R_{13}, f \circ R_{23}\}, \{R_{23}, f \circ R_{13}\}$
(t, f, t)	$\{R_1, f \circ R_{13}\}, \{R_2, f \circ R_{23}\}$
(6, 4, 2)	$\{R_{13}, f \circ R_1\}, \{R_{23}, f \circ R_2\}$
(o, e, e)	$\{R_1, f \circ R_1\}, \{R_2, f \circ R_2\}$
(5, 4, 2)	$\{R_{13}, f \circ R_{13}\}, \{R_{23}, f \circ R_{23}\}$
(f, t, t)	$\{R_1, R_{23}\}, \{f \circ R_1, f \circ R_{23}\}$
(8, 6, 2)	$\{R_2, R_{13}\}, \{f \circ R_2, f \circ R_{13}\}$
(f, t, f)	$\{R_1, R_2\}, \{f \circ R_1, f \circ R_2\}$
(8, 6, 4)	$\{R_{13}, R_{23}\}, \{f \circ R_{13}, f \circ R_{23}\}$
(f, f, t)	$\{R_1, R_{13}\}, \{f \circ R_1, f \circ R_{13}\}$
(8, 4, 2)	$\{R_2, R_{23}\}, \{f \circ R_2, f \circ R_{23}\}$

Table 11. Analogous of Table 10 for caustic type EH2.

(m_0, m_1, m_2) kind/minimal	Couples of reversors
(t, t, t)	$\{R, f \circ R_{123}\}, \{R_2, f \circ R_{13}\}$
(10, 6, 2)	$\{R_3, f \circ R_{12}\}, \{R_{23}, f \circ R_1\}$
(t, t, f)	$\{R, f \circ R_{12}\}, \{R_2, f \circ R_3\}$
(10, 6, 4)	$\{R_3, f \circ R_{123}\}, \{R_{23}, f \circ R_{13}\}$
(t, f, t)	$\{R, f \circ R_{13}\}, \{R_3, f \circ R_1\}$
(6, 4, 2)	$\{R_2, f \circ R_{123}\}, \{R_{23}, f \circ R_{12}\}$
(t, f, f)	$\{R, f \circ R_1\}, \{R_2, f \circ R_{12}\}$
(10, 8, 4)	$\{R_3, f \circ R_{13}\}, \{R_{23}, f \circ R_{123}\}$
(f, t, t)	$\{R, R_{23}\}, \{f \circ R_1, f \circ R_{123}\}$
(8, 6, 2)	$\{R_2, R_3\}, \{f \circ R_{12}, f \circ R_{13}\}$
(f, t, f)	$\{R, R_2\}, \{f \circ R_{13}, f \circ R_{123}\}$
(8, 6, 4)	$\{R_3, R_{23}\}, \{f \circ R_1, f \circ R_{12}\}$
(f, f, t)	$\{R, R_3\}, \{f \circ R_{12}, f \circ R_{123}\}$
(8, 4, 2)	$\{R_2, R_{23}\}, \{f \circ R_1, f \circ R_{13}\}$

Table 12. Analogous of Table 10 for caustic type H1H2.

(m_0, m_1, m_2) kind/minimal	Couples of reversors
(t, t, t) (10, 6, 2)	$(R_3 f \circ R_{12}), (R_2 f \circ R_{13})$ $(f \circ R_{12} R_3), (f \circ R_{13} R_2)$
(t, t, f) (10, 6, 4)	$(R_2 f \circ R_{12}), (R_3 f \circ R_{13})$ $(f \circ R_{12} R_2), (f \circ R_{13} R_3)$
(t, f, t) (6, 4, 2)	$(R_2, f \circ R_{13}), (R_2, f \circ R_{13})$ $(R_3, f \circ R_{12}), (R_3, f \circ R_{12})$
(t, f, f) (10, 8, 4)	$(R_2, f \circ R_{12}), (R_2, f \circ R_{12})$ $(R_3, f \circ R_{13}), (R_3, f \circ R_{13})$
(f, t, t) (8, 6, 2)	$(R_2 R_3), (f \circ R_{13} f \circ R_{12})$ $(R_3 R_2), (f \circ R_{12} f \circ R_{13})$
(e, o, e) (4, 3, 2)	$(R_2 R_2), (f \circ R_{12} f \circ R_{12})$ $(R_3 R_3), (f \circ R_{13} f \circ R_{13})$
(f, f, t) (8, 4, 2)	$(R_2, R_3), (f \circ R_{12}, f \circ R_{13})$ $(R_2, R_3), (f \circ R_{12}, f \circ R_{13})$

Table 13. Analogous of Table 10 for caustic type H1H1. See comments after the proof of Theorem 6 for the meaning of $(|)$.

We have seen that, once fixed the caustic type, there exists a tight relation between the symmetry sets associated to an SPT and the kind of winding numbers. A similar result for standard-like maps was obtained by Kook and Meiss in [22]. Compare Tables 10–13 with their Table I, where they list the 36 classes of SPOs for the 4D symplectic Froeschlé map. Our 4D symplectic billiard map has more classes because a new factor enters in the classification: the caustic type.

6.7 Gallery of minimal SPTs

We have 112 classes of SPTs listed in Tables 10–13, so we tackle the task of finding a minimal representative in each class. They have periods $m_0 \in \{4, 5, 6, 8, 10\}$.

The algorithm for the caustic type EH1 is: 1) Choose one of the seven minimal winding numbers (m_0, m_1, m_2) in Table 10; 2) Find caustic parameters $\lambda_1 \in E$ and $\lambda_2 \in H_1$ such that (13) holds; 3) Choose one of the four couples of reversors $\{r, \check{r}\}$ in the corresponding row of Table 10; 4) Get a point (q, p) from Table 7 using the reversor r (or \check{r}); and 5) Draw the doubly SPT through q with velocity p .

Only step 2) is problematic, because it requires the inversion of the frequency map. The main obstacle is that equation (13) might not have solution in $E \times H_1$ for some of the minimal winding numbers at hand. Nevertheless, it is proved in [5] that $\omega|_{E \times H_1}$ is a diffeomorphism and

$$\lim_{a_1 \rightarrow 0^+} \omega(E \times H_1) = \{(\omega_1, \omega_2) \in \mathbb{R}^2 : 0 < \omega_2 < \omega_1 < 1\}.$$

Consequently, equation (13) has a unique solution in $E \times H_1$ provided that ellipsoid (9) is flat enough.

The other three caustic types can be dealt with the same algorithm. There is just one difference among them. Namely, we must consider different shapes of ellipsoids to ensure that equation (13) has a solution. More precisely, we must consider almost flat ellipsoids — a_1 small— for caustic types EH1 and H1H1, and almost “segments” —both a_1 and a_2 small— for caustic types EH2 and H1H2. These results can be found in [5]. This explains why some ellipsoids in Tables 14–17 are so flat. We have chosen not too extreme ellipsoids whenever it has been possible.

We have found a minimal SPT of each class. Some of them are displayed in Tables 14–17. Arrows in their column headings point in the direction of increasing x_1 , x_2 or x_3 . Each line of the first three tables shows four different perspectives of an SPT. The 3D image corresponds to an isometric view of the first octant. The three projected planes are viewed from the positive missing axis. We only display 3D views in Table 17. Billiard trajectories are depicted in red. Green and yellow lines represent intersections of Q with H1-caustics and H2-caustics, respectively. The E-caustic is also shown in cases EH1 and EH2.

Period four takes only place for four classes of SPTs of type H1H1. Period five takes only place for eight classes of SPTs, half of type EH1 and half of type EH2. We display half of these minimal SPTs in Table 14. Their announced symmetries can be verified by observing their projections. We can check that trajectories of caustic type H1H1 give one turn around the x_1 -axis and have three tangential touches with the outer (respectively, inner) 1-sheet hyperboloid, trajectories of type EH1 give one turn around the x_1 -axis and cross four times the plane Π_1 , trajectories of type EH2 give two turns around the x_3 -axis and cross twice the plane Π_2 . This is consistent with the geometric interpretation given in Subsec. 6.2 of winding numbers.

We show in Table 15 the minimal representatives of the classes listed in the third row of Table 12. Since all of them have $(6, 4, 2)$ as winding numbers, they are 6-periodic, cross four times the plane Π_2 , and cross twice the plane Π_3 .

In Table 16 we present half of the 6-periodic minimal SPTs with an ellipsoidal caustic. They correspond to the third row of Tables 10–11.

Finally, we draw several SPTs of type H1H1 in Table 17. They show the difference among classes $(R_2 | R_2)$, $(R_3 | R_3)$, $(R_2, R_3 |)$, $(R_2 | R_3)$, $(R_3 | R_2)$, and $(| R_2, R_3)$. We can locate those classes in the last rows of Table 13. One can observe, for instance, that the SPT of class $(R_2, R_3 |)$ has two impacts on the intersection $Q \cap \Pi_2 \cap Q_{\lambda_1}$ and two more on $Q \cap \Pi_3 \cap Q_{\lambda_1}$. On the contrary, the SPT of class $(| R_2, R_3)$ has two impacts on the intersection $Q \cap \Pi_2 \cap Q_{\lambda_2}$ and two more on $Q \cap \Pi_3 \cap Q_{\lambda_2}$. Since $\lambda_1 < \lambda_2$, Q_{λ_1} and Q_{λ_2} are the outer and inner one-sheet hyperboloids, respectively.

Some comments about these trajectories are in order:

- The 4-periodic trajectories in Table 14 are the simplest examples of nonplanar periodic trajectories. Besides, they are one of the few simply SPTs. Both trajectories have two points on the same symmetry set. However, each point is associated to a different caustic: inner or outer. That property is easier to see in the first one. Hence, they are of class $(R_2 | R_2)$ and $(f \circ R_{13} | f \circ R_{13})$ in the notation used in Table 13.
- The 5-periodic trajectories in Table 14 are the simplest examples of nonplanar periodic trajectories with odd period. They have one point on a symmetry set and another on the associated symmetry set. We recall that only SPTs with odd period have this property; see item c) of Theorem 1.
- Many projections onto the horizontal plane Π_1 look like 2D SPTs (cf. Table 5).
- Any R -SPT is travelled twice in opposite directions, since it hits orthogonally the ellipsoid at some point $q \in Q \cap Q_{\lambda_1} \cap Q_{\lambda_2}$. Therefore, there exist SPTs of even

period $m_0 = 2l \geq 6$ with only $l + 1$ distinct impact points on the ellipsoid, although all of them are of

caustic type H1H2. We show a 6-periodic sample (the simplest one) in the first row of Table 15.

3D ($x_1: \uparrow, x_2: \searrow, x_3: \swarrow$)	Plane Π_1 ($x_2: \uparrow, x_3: \rightarrow$)	Plane Π_2 ($x_1: \uparrow, x_3: \leftarrow$)	Plane Π_3 ($x_1: \uparrow, x_2: \rightarrow$)	Data
				H1H1 (4, 3, 2) 0.8 0.13 0.648376 0.130077 R_2
				H1H1 (4, 3, 2) 0.8 0.13 0.648376 0.130077 $f \circ R_{13}$
				EH2 (5, 4, 2) 0.3969 0.2 0.762965 0.199523 R_1 $f \circ R_1$
				EH2 (5, 4, 2) 0.3969 0.2 0.762965 0.199523 R_{23} $f \circ R_{23}$
				EH1 (5, 4, 2) 0.49 0.25 0.260266 0.231635 R_{12} $f \circ R_{12}$
				EH1 (5, 4, 2) 0.49 0.25 0.260266 0.231635 R_3 $f \circ R_3$

Table 14. Two minimal SPTs of period 4 and four minimal SPTs of period 5. The “Data” column includes consecutively: caustic type, winding numbers (m_0, m_1, m_2) , ellipsoid parameters a_2 and a_1 —we have set $a_3 = 1$ —, caustic parameters λ_2 and λ_1 , and all reversors whose symmetry sets intersect the corresponding SPOs.

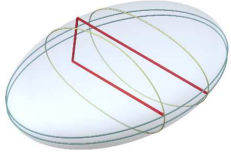
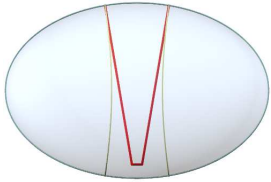
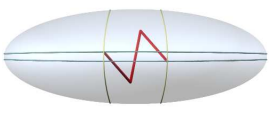
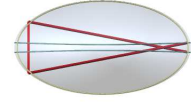
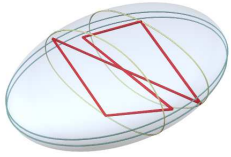
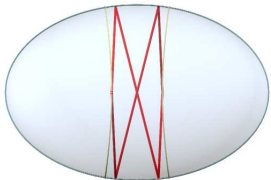
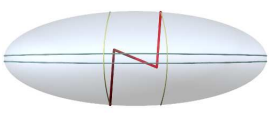
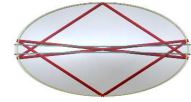
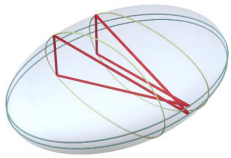
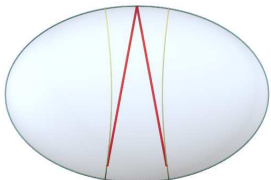
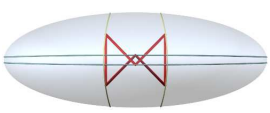
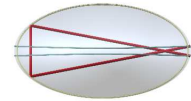
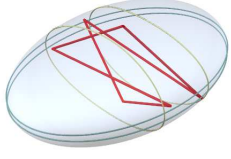
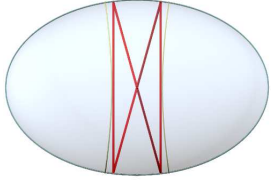
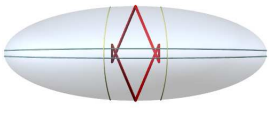
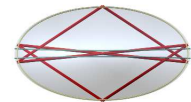
3D ($x_1: \uparrow, x_2: \searrow, x_3: \swarrow$)	Plane Π_1 ($x_2: \uparrow, x_3: \rightarrow$)	Plane Π_2 ($x_1: \uparrow, x_3: \leftarrow$)	Plane Π_3 ($x_1: \uparrow, x_2: \rightarrow$)	Data
				H1H2 (6, 4, 2) 0.45 0.13 0.967756 0.133273 R $f \circ R_{13}$
				H1H2 (6, 4, 2) 0.45 0.13 0.967756 0.133273 R_2 $f \circ R_{123}$
				H1H2 (6, 4, 2) 0.45 0.13 0.967756 0.133273 R_3 $f \circ R_1$
				H1H2 (6, 4, 2) 0.45 0.13 0.967756 0.133273 R_{23} $f \circ R_{12}$

Table 15. The four classes of SPTs with minimal winding numbers $(m_0, m_1, m_1) = (6, 4, 2)$ and H1H2-caustics. “Data” column as in Table 14.

7 The general case

We have characterized STs and SPTs in terms of the vertexes of some rectangles (for the 2D case) and cuboids (for the 3D case). We have proved that there are exactly 12 and 112 classes of SPTs in these low-dimensional cases. See Theorem 5 and Theorem 6.

Next, we generalize both characterizations and the final classification to nondegenerate ellipsoids of \mathbb{R}^{n+1} .

We say that two SPTs are of the same class when both SPTs have the same type of caustics and they connect the same couple of vertexes of their respective cuboids. All SPTs inside the same class are associated to the same reversors. For instance, looking at Table 4 and the last column of Table 5, we see that all SPTs whose type of caustic is E and that connect the two left (respectively, right) vertexes of the rectangle \mathcal{C}_λ are associated to the reversors R_x and R_y (respectively, $f \circ R_x$ and $f \circ R_y$).

We have the following result.

Theorem 7. *Nonsingular STs (respectively, nonsingular SPTs) inside nondegenerate ellipsoids of \mathbb{R}^{n+1} are characterized as trajectories passing, in elliptic coordi-*

nates, through some vertex (respectively, two different vertexes) of their cuboid. All nonsingular SPOs are doubly SPOs, but a few with caustics of repeated types. There are $2^{2n}(2^{n+1} - 1)$ classes of nonsingular SPTs.

This theorem is obtained by means of small refinements of the techniques used in this article, although some checks become rather cumbersome.

The number $2^{2n}(2^{n+1} - 1)$ has a simple explanation. There are 2^n types of caustics —see remark 3—, and any $(n + 1)$ -dimensional cuboid has 2^{n+1} vertexes, and so $2^n(2^{n+1} - 1)$ couples of vertexes.

Once fixed the ellipsoid and the caustic type, all $2^n(2^{n+1} - 1)$ couples of vertexes are *realizable*. That is, each couple is connected by some SPT. Of course, one should choose suitable winding numbers for each couple. That choice is guided by the following observation.

Let \mathcal{C}_λ be a cuboid such that its billiard trajectories are periodic with winding numbers m_0, \dots, m_n . Let $\hat{q} = (\hat{\mu}_0, \dots, \hat{\mu}_n)$ and $\tilde{q} = (\tilde{\mu}_0, \dots, \tilde{\mu}_n)$ be any couple of different vertexes of \mathcal{C}_λ connected by an SPT. If some winding number is odd, then $\hat{\mu}_i = \tilde{\mu}_i \Leftrightarrow m_i \in 2\mathbb{Z}$ for $i = 0, \dots, n$. If all winding numbers are even, then $\hat{\mu}_i = \tilde{\mu}_i \Leftrightarrow m_i \in 4\mathbb{Z}$ for $i = 0, \dots, n$.

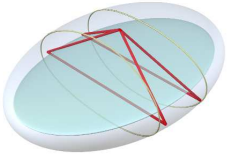
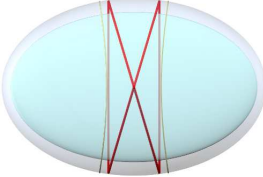
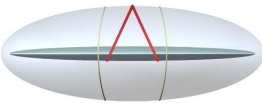

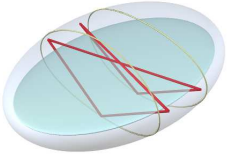
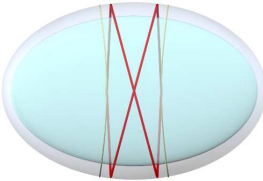
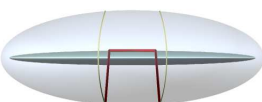

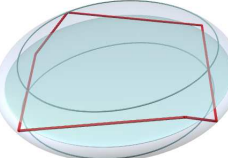
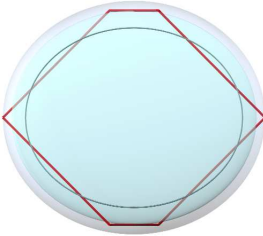
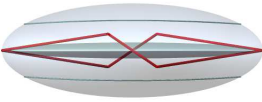
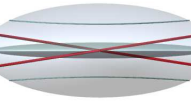
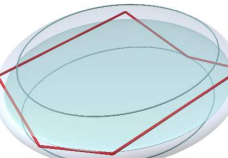
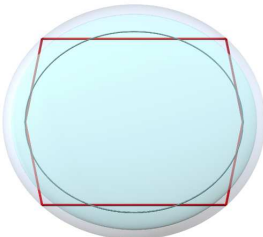

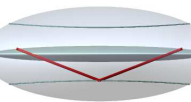
3D ($x_1: \uparrow, x_2: \searrow, x_3: \swarrow$)	Plane Π_1 ($x_2: \uparrow, x_3: \rightarrow$)	Plane Π_2 ($x_1: \uparrow, x_3: \leftarrow$)	Plane Π_3 ($x_1: \uparrow, x_2: \rightarrow$)	Orbit data
				EH2 (6, 4, 2) 0.45 0.13 0.962896 0.126968 R_{23} $f \circ R_2$
				EH2 (6, 4, 2) 0.45 0.13 0.962896 0.126968 R_2 $f \circ R_{23}$
				EH1 (6, 4, 2) 0.8 0.13 0.403278 0.126231 R_{12} $f \circ R_{13}$
				EH1 (6, 4, 2) 0.8 0.13 0.403278 0.126231 R_2 $f \circ R_3$

Table 16. Four minimal SPTs with winding numbers $(m_0, m_1, m_2) = (6, 4, 2)$ and an ellipsoidal caustic. “Data” as in Table 14.

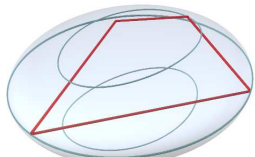
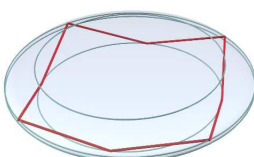
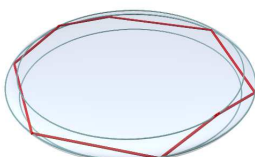
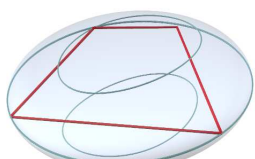
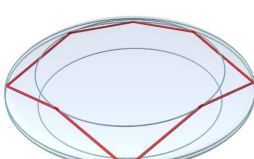
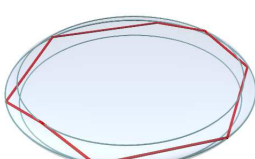
3D ($x_1: \uparrow, x_2: \searrow, x_3: \swarrow$)	Data	3D ($x_1: \uparrow, x_2: \searrow, x_3: \swarrow$)	Data	3D ($x_1: \uparrow, x_2: \searrow, x_3: \swarrow$)	Data
	H1H1 (4, 3, 2) 0.8 0.13 0.648376 0.130077 ($R_2 R_2$)		H1H1 (8, 4, 2) 0.95 0.05 0.056134 0.457414 ($R_2, R_3 $)		H1H1 (8, 6, 2) 0.95 0.05 0.050041 0.229595 ($R_2 R_3$)
	H1H1 (4, 3, 2) 0.8 0.13 0.648376 0.130077 ($R_3 R_3$)		H1H1 (8, 4, 2) 0.95 0.05 0.056134 0.457414 ($ R_2, R_3$)		H1H1 (8, 6, 2) 0.95 0.05 0.050041 0.229595 ($R_3 R_2$)

Table 17. Six SPTs (3D view) for H1H1-caustics. They show different classes of SPTs corresponding to reversors R_2 and/or R_3 . “Data” as in Table 14.

8 Conclusions and future work

We have shown that the billiard map associated to a convex symmetric hypersurface $Q \subset \mathbb{R}^{n+1}$ is reversible. Even more, it admits 2^{n+1} factorizations as a composition of two involutions. Therefore, its SPOs can be classified by the symmetry sets they meet. We have carried out this classification for nondegenerate ellipsoids of \mathbb{R}^{n+1} . The characterization of STs and SPTs in terms of their elliptic coordinates has been the key tool.

The existence of SPOs is useful for several reasons. We indicate just two.

First, it reduces the numerical computations needed to find them. Concretely, we can halve the dimension of the problem, by restricting the search of periodic points on the n -dimensional symmetry sets. (This issue will be greatly appreciated when dealing with perturbed ellipsoids, for which no frequency map exists, since the integrability is lost.) Second, an SPO of a completely integrable reversible map, persists under symmetric perturbations, when the symmetry sets are transverse to the Liouville invariant tori of the map at some point of the SPO.

These two facts are crucial to study billiards inside symmetrically perturbed ellipsoids, which is our next goal. To be more precise, we plan to generalize the results about the break-up of resonant invariant curves for billiards inside perturbed circles [27] and perturbed ellipses [10].

Bibliography

- [1] ABENDA, S., AND FEDOROV, Y. Closed geodesics and billiards on quadrics related to elliptic KdV solutions. *Lett. Math. Phys.* 76 (2006), 111–134.
- [2] BABENKO, I. K. Periodic trajectories in three-dimensional Birkhoff billiards. *Math. USSR-Sb.* 71, 1 (1992), 1–13.
- [3] BERGER, M. Seules les quadriques admettent des caustiques. *Bull. Soc. Math. France* 123 (1995), 107–116.
- [4] BIRKHOFF, G. D. *Dynamical Systems*, vol. IX of *Amer. Math. Soc. Colloq. Publ.* AMS, Providence, RI, 1966.
- [5] CASAS, P. S., AND RAMÍREZ-ROS, R. The frequency map for billiards inside ellipsoids. *SIAM J. Appl. Dyn. Syst.* 10, 1 (2011), 278–324.
- [6] CAYLEY, A. Developments on the porism of the in-and-circumscribed polygon. *Philos. Mag.* 7 (1854), 339–345.
- [7] CHANG, S. J., CRESPI, B., AND SHI, K. J. Elliptical billiard systems and the full Poncelet’s theorem in n dimensions. *J. Math. Phys.* 34 (1993), 2242–2256.
- [8] CHANG, S. J., CRESPI, B., AND SHI, K. J. Elliptical billiards and hyperelliptic functions. *J. Math. Phys.* 34 (1993), 2257–2289.
- [9] CHANG, S. J., AND FRIEDBERG, R. Elliptical billiards and Poncelet’s theorem. *J. Math. Phys.* 29 (1988), 1537–1550.
- [10] DE CARVALHO, S. P., AND RAMÍREZ-ROS, R. Nonpersistence of resonant caustics in perturbed elliptic billiards. Preprint electronically available at [arXiv:1108.5582](https://arxiv.org/abs/1108.5582), 2011.
- [11] DRAGOVIĆ, V., AND RADNOVIĆ, M. Conditions of Cayley’s type for ellipsoidal billiard. *J. Math. Phys.* 39 (1998), 355–362.
- [12] DRAGOVIĆ, V., AND RADNOVIĆ, M. On periodical trajectories of the billiard systems within an ellipsoid in R^d and generalized Cayley’s condition. *J. Math. Phys.* 39 (1998), 5866–5869.
- [13] DRAGOVIĆ, V., AND RADNOVIĆ, M. Geometry of integrable billiards and pencils of quadrics. *J. Mathématiques Pures Appliquées* 85, 6 (2006), 758–790.
- [14] DRAGOVIĆ, V., AND RADNOVIĆ, M. Bifurcations of Liouville tori in elliptical billiards. *Regul. Chaotic Dyn.* 14 (2009), 479–494.
- [15] FARBER, M. Topology of billiard problems, I. *Duke Math. J.* 115, 3 (2002), 559–585.
- [16] FARBER, M. Topology of billiard problems, II. *Duke Math. J.* 115, 3 (2002), 587–621.
- [17] FARBER, M., AND TABACHNIKOV, S. Periodic trajectories in 3-dimensional convex billiards. *Manuscripta Math.* 108, 4 (2002), 431–437.
- [18] FEDOROV, Y. Classical integrable systems and billiards related to generalized Jacobians. *Acta Appl. Math.* 55 (1999), 251–301.
- [19] FEDOROV, Y. Algebraic closed geodesics on a triaxial ellipsoid. *Regul. Chaotic Dyn.* 10 (2005), 463–485.
- [20] GRAMCHEV, T., AND POPOV, G. Nekhoroshev type estimates for billiard ball maps. *Ann. Inst. Fourier (Grenoble)* 45 (1995), 859–895.
- [21] GRUBER, P. M. Only ellipsoids have caustics. *Math. Ann.* 303 (1995), 185–194.
- [22] KOOK, H., AND MEISS, J. D. Periodic orbits for reversible, symplectic mappings. *Phys. D* 35, 1-2 (1989), 65–86.
- [23] KOZLOV, V. V., AND TRESHCHĚV, D. *Billiards: a Genetic Introduction to the Dynamics of Systems with Impacts*. AMS, 1991.
- [24] LAMB, J. S. W., AND ROBERTS, J. A. G. Time-reversal symmetry in dynamical systems: a survey. *Phys. D* 112, 1-2 (1998), 1–39.
- [25] MOSER, J., AND VESELOV, A. P. Discrete versions of some classical integrable systems and factorization of matrix polynomials. *Commun. Math. Phys.* 139 (1991), 217–243.
- [26] PONCELET, J. V. *Traité des Propriétés Projectives des Figures*. Bachelier, Paris, 1822.
- [27] RAMÍREZ-ROS, R. Break-up of resonant invariant curves in billiards and dual billiards associated to perturbed circular tables. *Phys. D* 214, 1 (2006), 78–87.
- [28] TABACHNIKOV, S. *Billiards*. Société Mathématique de France, 1995.
- [29] TABACHNIKOV, S. *Geometry and Billiards*. AMS, 2005.
- [30] VESELOV, A. P. Integrable systems with discrete time and difference operators. *Funct. Anal. Appl.* 22, 2 (1988), 1–13.
- [31] WAALKENS, H., AND DULLIN, H. R. Quantum monodromy in prolate ellipsoidal billiards. *Ann. Phys. (NY)* 295 (2002), 81–111.
- [32] WAALKENS, H., WIERSIG, J., AND DULLIN, H. R. Triaxial ellipsoidal quantum billiards. *Ann. Phys. (NY)* 276 (1999), 64–110.